Where Rivers Meet: Landscape, Ritual, Settlement and the Archaeology of River Gravels

Aggregates Levy Sustainability Fund

Catholme Ceremonial Complex Geophysical Data Report for Magnetic Properties

Mark W. Hounslow & Vassil Karloukovski
Centre for Environmental Magnetism and Palaeomagnetism
Geography Dept., Lancaster Environment Centre,
Lancaster University.

m.hounslow@lancs.ac.uk
http://geography.lancs.ac.uk/cemp/cemp.htm

March. 24th, 2005.

Summary

- There is not a large contrast in the *in situ* magnetisation properties of the various types of archaeological features on the site. There is a broad spread of magnetisation intensity values which range from relatively weakly magnetic pit alignment features to shallow pit and large pit features which are more strongly magnetic. The strongest magnetic materials on the site are features associated with *in situ* burning, which are about 1 order of magnitude more magnetic than other archaeological fills.
- The magnetic mineral properties of the archaeological fills from the site appear to be strongly influenced by the presence of burnt materials. These appear to have a distinctively large frequency dependent magnetic susceptibility, which is larger than the plough-soil on the site.
- Some post pit features have unusually large frequency dependent magnetic susceptibility values, which are suggestive of either unusual ground conditions, stimulated by wood decomposition, or unusual sources of burnt material. Pit alignment features have unusually low frequency dependent magnetic susceptibility and magnetic susceptibility suggesting the content of these archaeological fills is quite different to the other types of archaeological fills.
- Most of the archaeological fills display an erratic decrease downwards from the sub-soil surface, in the strength of their magnetic susceptibility and remanence.
- The remanent magnetisation of all materials is dominated by a viscous (time-dependent) magnetisation.
- Corrections for this viscous magnetisation applied to the specimens, indicates that the *in situ* natural remanence in archaeological fills is some 20 to 50% larger than the remanence measured 1 day after collection of the specimens. This range falls to 20 to 40% for the underlying Holocene sands.
- The *in situ* magnetisation is equal to or mostly larger than the induced magnetisation caused by the magnetic susceptibility, so that remanence intensity

is equally important, or more so, than the magnetic susceptibility for controlling survey magnetic anomalies. Pit alignments, regular pits and linear ditch features have fills in which the remanence intensity is 2 to 4 times more important than the induced magnetisation in controlling the total magnetisation intensity. On average other types of features have values from 0.5 to 1, with burnt features typically being dominated by induced magnetisation anomalies.

- In magnetic gradiometer surveys the importance of the strong viscous remanence will dictate the degree of masking caused by recently ploughed soil to the identification of archaeological features. Less recently ploughed and disturbed soils should give better definition of archaeological features. This may explain the differences in identification of archaeological anomalies in fields F1 and B2, by the two soil-surface magnetic surveys.
- The geological materials on the site display substantive variations in magnetic properties, which in some circumstances will produce gradiometer anomalies. The magnetic properties of the sandy geological materials overlap with the more weakly magnetic archaeological materials. On a large scale, differences in the sand to gravel ratio could contribute to some magnetic anomalies, since the gravel-dominated lenses in the Holocene sands will have a near zero induced and remanent magnetisation.
- For some types of features, sampling predominantly located at the sub-soil level (level at which soil stripped off), has probably introduced some bias in the magnetic properties determined. This is due to the strong depth-related changes in magnetic properties.
- Some simple forward modelling of selected magnetic anomalies indicates that there is not a particularly good correspondence between the calculated and measured gradient-field anomalies, particularly for the G858 magnetometer. This may be due to a variety of reasons, such as a) inadequate information on soil-depth over features which have been surveyed at soil-level, b) inadequacies of the simple modelling utilised, c) overestimation of magnetisation intensity for some features due to lack of information on the vertical variation in magnetisation intensity of the fills, d) inadequate estimation of the magnetisation background values from the Holocene sands adjacent to the features modelled.
- Any follow-up work should focus on a) better characterisation and understanding of the source of the magnetically enhanced burnt material- relationships with charcoal abundance should be sought to verify this; b) isolating the reasons for the mismatch between actual measured anomalies and the forward modelling from the magnetic properties.

Contents:

1. Aims of magnetic properties subproject

The aims of this sub-project has been to:

a) characterise the magnetic properties of the Catholme site materials, so that robust predictive determinations of the remanent and induced magnetisations could be done at the site. This predictive approach was designed to produce realistic estimates of the likely magnetic properties of materials on areas of the site for which no samples had been taken. This would naturally require linking into a functional classification of archaeological features, and magnetic anomaly types on the site. Ultimately (in the future) this data could be used for robust numerical modelling of the magnetic anomalies on the site.
b) provide a better fundamental understanding of the reasons for variations in the magnetic properties, and the variable detection of archaeological features on the site through magnetic geophysical surveys. This links with the micromorphological work being undertaken.

2. Magnetic properties and geophysical magnetic anomalies

Two types of magnetic properties of archaeological materials control the size and form of the magnetic anomalies in a magnetic survey. In a mathematical sense, the anomalies measured by a geophysical magnetic survey are a complex function of the 3-dimensional variation in the induced magnetisation J_i, and the remanent magnetisation J_r of the site materials.

2.1 Magnetic susceptibility.

Magnetic susceptibility χ controls the magnitude of the magnetisation induced (J_i) by the earths magnetic field through the relationship $J_i = \chi . H$, where H is the earths magnetic field. It is the 3-dimensional variations in the magnetic susceptibility that in part controls the form and magnitude of the anomalies measured by magnetic geophysical survey. The magnetic susceptibility is a measure of the abundance of the various types of magnetic mineral particles. This property can either be measured *in situ*, or with greater sensitivity using equipment in the laboratory.

2.2 Remanent magnetisation intensity.

This is the permanent magnetisation (remanence) which is carried by the material, the property is expressed as both magnitude and direction. This remanence may be produced in a variety of ways:

a) heating of the materials *in situ* to produce a thermoremanence (TRM), in the direction of the earths magnetic field at the time of heating.
b) Chemical remanent magnetisation (CRM) produced through production of new magnetic minerals *in situ* at the site, and their subsequent growth in size so that they pass the threshold for remanence acquisition. This process can occur in some types of waterlogged ditchs (i.e. with anoxic fills) and in soils.
c) Depositional remanent magnetisation (DRM) which may be produced when the sediment is deposited in the archaeological feature, either through water or wind transport, or perhaps through direct human transference. The material acquires this remanence magnetisation in the direction of the earths magnetic field at the time of its deposition. Mineral grains which may have acquired a CRM or TRM

elsewhere may be subsequently dispersed over the site and acquire a DRM at their final resting place. For example materials from hearths or burn-sites.

d) Viscous remanent magnetisation (VRM), which is a time-dependent remanence, which may be acquired once the sediment/soil is *in situ*. This VRM will at any one time be acquired in the direction of the earths magnetic field at that time. Removing a sample from its *in situ* position will cause a progressive time-dependent loss of the VRM that has been acquired *in situ*. This is referred to as VRM loss or decay.

Various types of magnetometers measure remanent magnetisation. These all require an oriented sample to be prepared and inserted into the magnetometer. In an ideal world it would have been preferable to measure the remanent magnetisation of the site materials very close to their time of sampling, to minimise the effect of VRM loss. However, it was not logistically possible to assess the *in situ* remanent magnetisation, using a magnetometer in the field. Hence, the major part of the project has been to estimate the *in situ* remanence (NRM_0) by determining the amount of VRM decay. This is determined by measuring the remanent magnetisation one day after measurement (NRM_1), and determine the amount of VRM lost (VRM_1) from collection to first measurement (Appendix 1). This concept can be expressed by the vector equation:

$$\mathbf{NRM_0 = VRM_1 + NRM_1}$$

3 Sampling

3.1 Rationale

The sampling strategy was based around three objectives:

- To provide as many representative archaeological and magnetic anomaly features on the site, given the limited budget, so that it was possible to obtain a database of the full range of likely magnetic material properties. These samples were collected after discussion with the various other sub-project participants, so as to maximise the integration of datasets. This sampling also included the geological features, some of which were significant for producing magnetic anomalies. The sampling also included some plough (top) soils, since the soil may mask significant archaeological features during magnetic surveys. Both vertical and horizontal profiling was used, depending upon the nature and extent of the archaeological feature, and the availability of suitable materials at the site on the various site visits. These represented the bulk of the work reported here.
- A set of samples to understand the variation of magnetic susceptibility with particle size in the various types of features on the site. This would help in understanding the location of the magnetic mineral grains, responsible for the magnetic properties, as well as a potentially predictive tool to apply to unsampled deposits.
- A set of samples to cross-calibrate the in situ magnetic susceptibility measurements and the laboratory magnetic susceptibility measurements.

3.2 The oriented samples for remanence determination

A total of 178 samples were collected during five consecutive trips to the Catholme site (φ=52.744^o, λ=358.29^o). These samplings were from fields A1, A2, B2, and F1, between August and October 2004. The samples were carefully prepared at the site to fit inside small cubic-plastic sample boxes. These boxes were orientated in the field using a magnetic compass and a device for measuring the dip of the front face of the plastic cubes. These dip and orientation values were used for correcting the measured remanent magnetisation back into *in situ* coordinates, once measured in the magnetometer. The plastic sample containers were sealed at the site to reduce moisture loss.

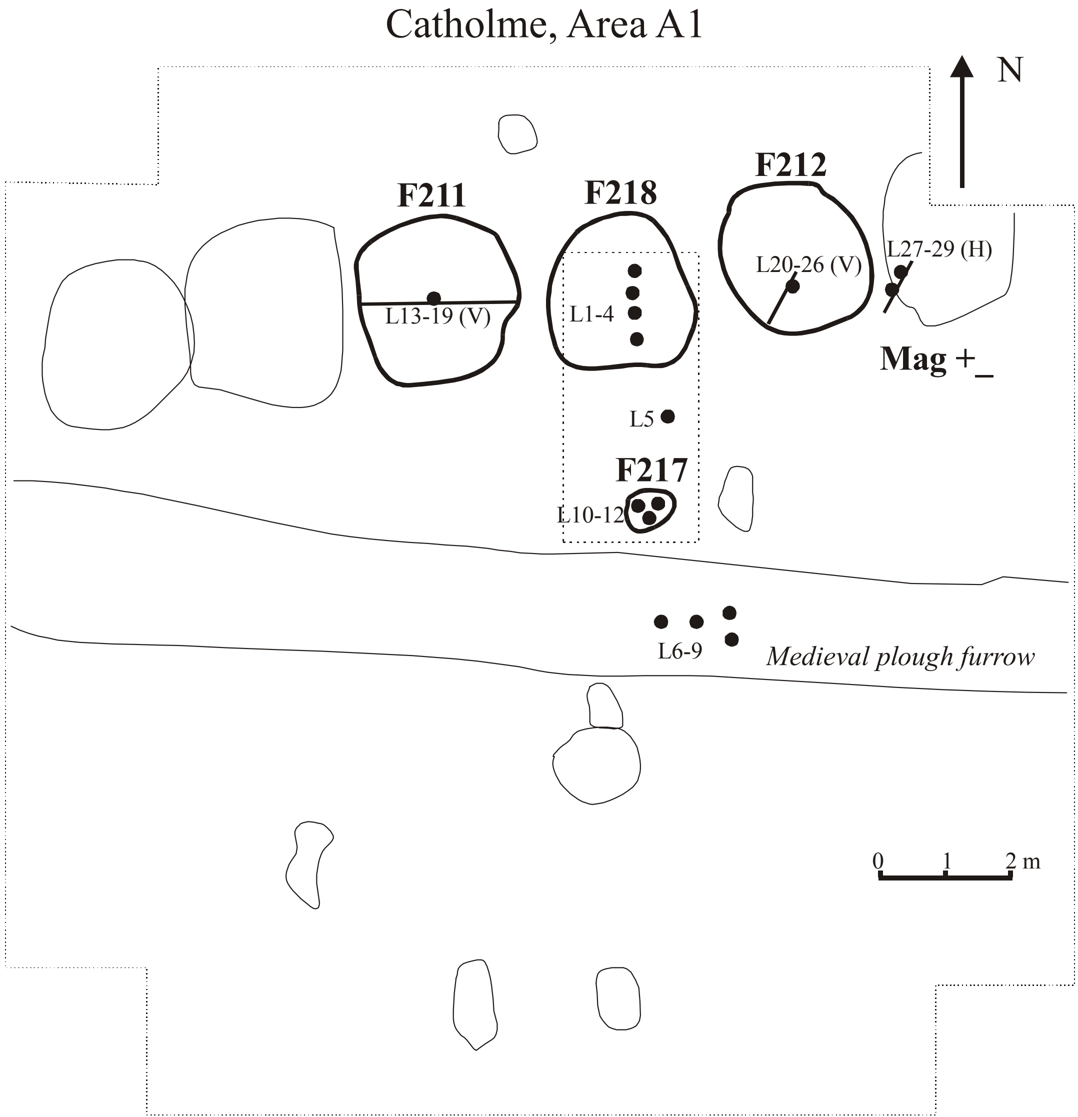

Figure 1 Sketch of the sampled features (bold lines) in area A1 at Catholme. The sample positions, L1 to L29, are shown. Specimens collected in a vertical (V), horizontal (H) or at sub-soil level(no ()) are indicated.

Figures 1 to 4 show the specimen positions placed onto the archaeological plans of fields A1, A2, B2, and F1. Table 1 lists the specimens according to the field and the archaeological features they were collected from. The specimens were collected either from vertical or horizontal traverses through the archaeological fills, or at the sub-soil level (level at which the soil was stripped off). The samples from the geological features of the site can be broadly classified into top-soils, plough furrows, Holocene sands which underlie the site and gravel clasts from the Holocene sands.

Table 1. List of all samples according to their field of collection. N – number of specimens per feature; 'Unassigned' refers to samples from archaeological features which were not excavated and hence were not given feature numbers. 'Geology' refers to the Holocene sands/gravels/top- soils sampled in proximity to the archaeological features.

Field	**Archaeological feature**	**N**	**Samples**	**Collected as:**
A1	F211	6	A1-L13, L14, L15, L16, L17, L18	vertical profile
	F212	7	A1-L20, L21, L22, L23, L24, L25, L26	vertical profile
	F217	3	A1-L10, L11, L12	at sub-soil level
	F218	4	A1-L1, L2, L3, L4	at sub-soil level
	MAG ±	3	A1-L27, L28, L29	horizontal profile
	Unassigned	4	A1-L6, L7, L8, L9	at sub-soil level
	Geology	2	A1-L5, L19	at sub-soil level
A2	F221	4	A2-L5, L6, L7, L8	at sub-soil level
	F223	18	A2-L9, L10, L11, L12, L13, L14, L15; A2-L24, L25, L26, L27, L28, L29; A2-L30, L31, L32, L33, L34	at sub-soil level; " horizontal profile; vertical profile
	F234	6	A2-L37, L38, L39, L40, L41, L42	vertical profile
	F241	4	A1-L1, L2, L3, L4	at sub-soil level
	Unassigned	6	A2-L18, L19, L20, L21, L22, L23	at sub-soil level
	Geology	7	A2-L16, L17; A2-L35, L36, L43, L44, L45	at sub-soil level; vertical profiles
B2	F105.08	4	B2-L67, L68, L72, L73	horizontal profile
	F105.10	13	B2-L4, L5, L10, L11, L12, L13; B2- L28, L29, L30, L31, L32, L33, L34	at sub-soil level; vertical profile "
	F105.11	4	B2-L35, L36, L37, L38	vertical profile
	F118	2	B2-L8, L9	at sub-soil level
	F126	14	B2-L1, L2, L3; B2-L54, L55, L56, L57, L58, L59, L60, 61; B2-L62, L63, L64	at sub-soil level; horizontal profile; vertical profile
	F134	2	B2-L6, L7	at sub-soil level
	F141	2	B2-L17, L18	at sub-soil level
	Geology	32	B2-L14, L15, L16, L19, L20, L21, L22, L23, L24, L25, L26, L27, L39, L40, L41, L42, L74, L75, L76; B2-L43, L44, L45, L46, L47, L48, L49, L50, L69, L70, L71; B2-L65, L66	at sub-soil level; " " horizontal profiles; " vertical profile
F1	F315	6	F1-L26, L27, L28, L29, L30, L31	horizontal and vertical profiles
	F317	5	F1-L5, L6, L7, L8, L9	vertical profile
	F320	5	F1-L10, L11, L12, L13, L14	horizontal profile
	F321	4	F1-L22, L23, L24, L25	horizontal profile
	F324	4	F1-L1, L2, L3, L4	vertical profile
	Geology	7	F1-L15, L16, L17, L18, L19, L20, L21	horizontal profiles

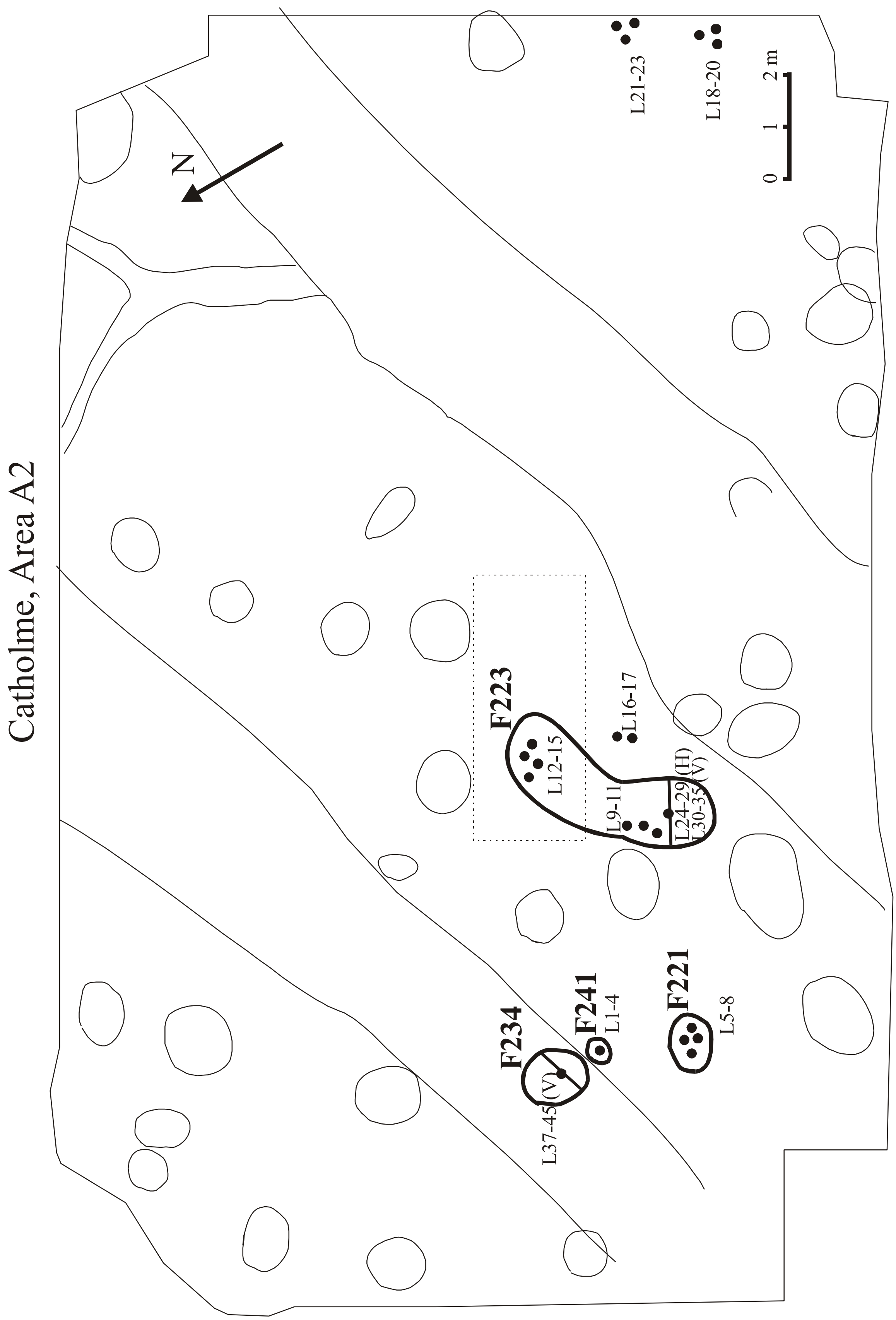

Figure 2. Sketch of the sampled features in area A2. See Fig. 1 for key.

.

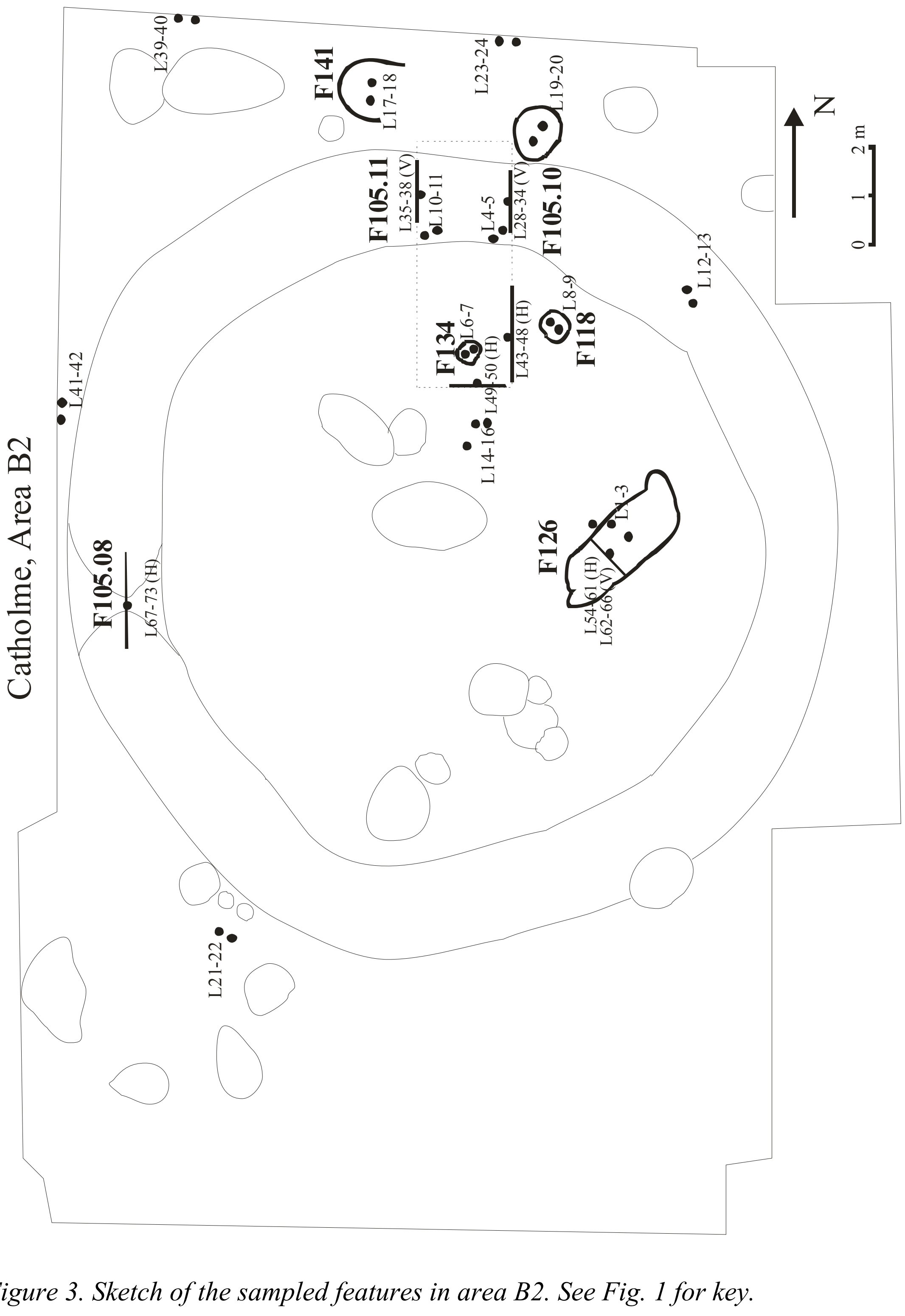

Figure 3. Sketch of the sampled features in area B2. See Fig. 1 for key.

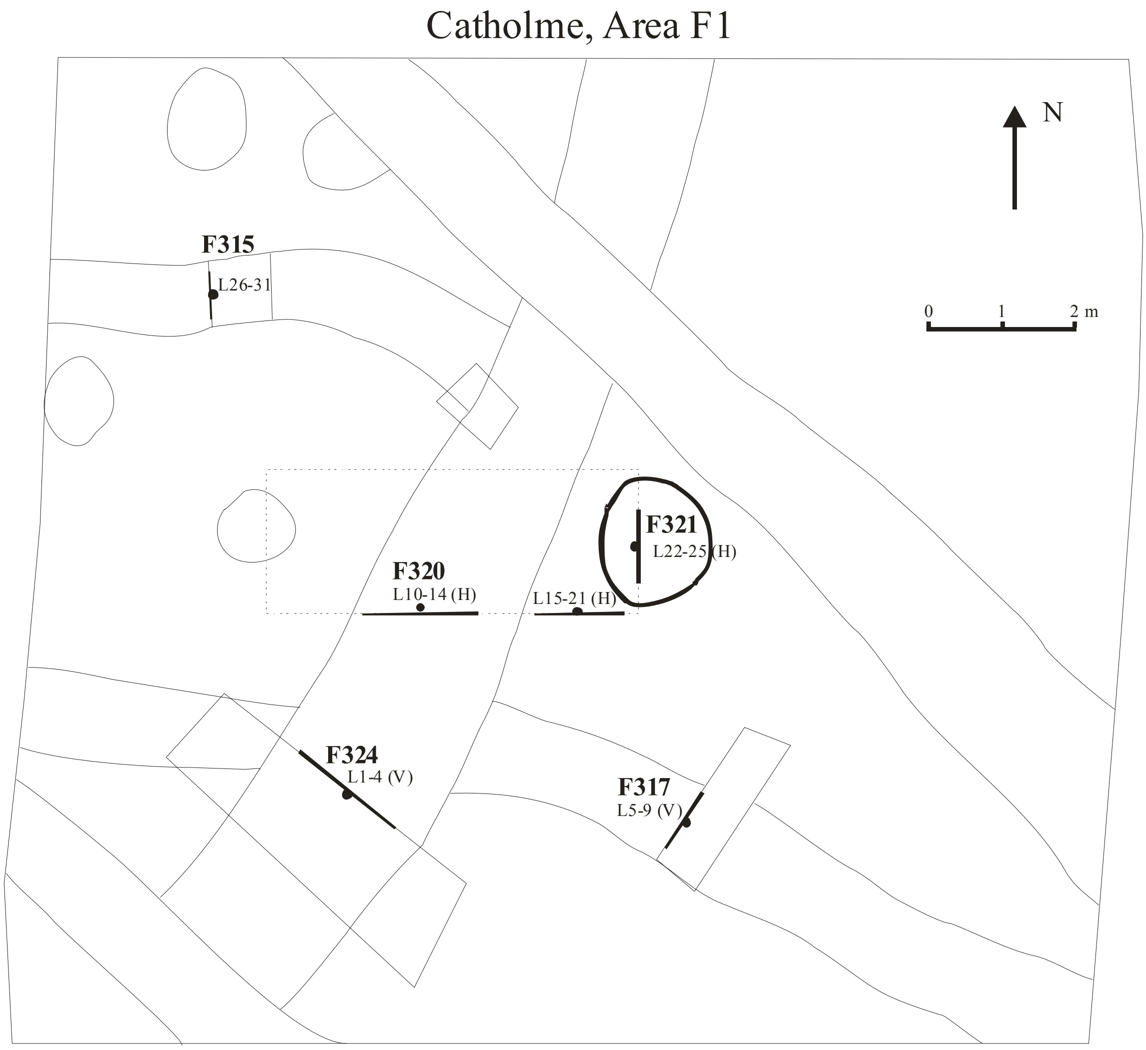

Figure 4. Sketch of the sampled features in area F1. See Fig. 1 for key.

The sampling was also classified according to the interpretation of the archaeological function of the sampled feature (Table 2). The classification of the archaeological function (Group A) was following that provided by S. Buteux and K. Bain, with additional classes for the non-archaeological features.

3.3 Other Sample Sets

Seven samples were collected to investigate the relationship between the magnetic susceptibility and grain size (Table 3). These cover a representative range of materials and archaeological features on the site.

A set of 27 samples were collected from fields A1, A2, and F1, in order to cross calibrate the magnetic susceptibility measurements performed at the site by Meg Watters, with those done in the Lancaster laboratory. The low-frequency magnetic susceptibility χ_{LF} of the sub-samples was measured *in situ* using a Bartington meter with a MS2F probe.

Table 2. List of all samples according to the type of interpreted function

Classification	N	Specimens / (*Field. Feature numbers*)
Archaeological functions		
Timber Post Pits	18	A2-L5, L6, L7, L8, L18, L19, L20, L21, L22, L23, L37, L38, L39, L40, L41, L42 / (*A2.F221, F234*) B2-L6, L7 / (*B2.F134*)
Pit alignment	20	A1-L1, L2, L3, L4, L10, L11, L12, L13, L14, L15, L16, L17, L18, L20, L21, L22, L23, L24, L25, L26 / (*A1.F218, F217, F211, F212*)
Linear Ditch	11	F1-L5, L6, L7, L8, L9, L26, L27, L28, L29, L30, L31 / (*F1.F317, F315*)
Ring Ditch	30	B2-L4, L5, L10, L11, L12, L13, L28, L29, L30, L31, L32, L33, L34, L35, L36, L37, L38, L67, L68, L72, L73 / (*B2.F105*) F1-L1, L2, L3, L4, L10, L11, L12, L13, L14 / (*F1.F324, F320*)
Regular pits	5	B2-L17, B2-L18, (*B2. F126*) F1-L22, L23, L24, L25 / (*F1.F321*)
Shallow Pit	6	A2-L1, L2, L3, L4 / (*A2.F241*) B2-L8, L9 / (*B2.F118*)
Huge Pit	18	A2-L9, L10, L11, L12, L13, L14, L15, L24, L25, L26, L27, L28, L29, L30, L31, L32, L33, L34 / (*A2.F223*)
Burnt features (Regular pit)	12	B2-L1, B2-L2, B2-L3, B2-L55, B2-L56, B2-L57, B2-L58, B2-L59, B2-L60, B2-L62, B2-L63, B2-L64 (*B2.F126*)
Other functions and groups:		
Modern top-soil	8	B2-L21, L22, L23, L24, L39, L40, L41, L42
Plough Furrow	4	A1-L6, L7, L8, L9
Holocene sands	36	A1-L5, L19, L27, L28, L29 A2-L16, L17, L35, L43, L44, L45 B2-L14, L15, L16, L19, L20, L43, L44, L45, L46, L47, L48, L49, L50, L65, L66, L69, L70, L71 F1-L15, L16, L17, L18, L19, L20, L21
Holocene gravel clasts	7	A2-L36 B2-L25, L26, L27, L74, L75, L76

Table 3. Samples used in the grain size analysis

Sample [feature]	Feature type/function
A1 [F211]	Pit alignment
A1 MAG±	Sandy gravel from a pronounced magnetic anomaly in field A1 (See Fig. 1).
A2 PS	Modern plough soil
A2 UG	Holocene sands
A2 [F238]	Post pit
B2 [F105.06]	Ring ditch
B2 [F126]	Regular pit

4. Methodology

4.1 Magnetic susceptibility.

The low and high-frequency field magnetic susceptibilities (χ_{LF} and χ_{HF}), were measured on a Bartington MS2 susceptibility meter (Appendix 5). As many of the samples were weakly magnetic, the more precise 6 measurement cycles routine described in Walden et al. (1999) was used throughout.

The percentage of frequency-dependant susceptibility $\%\chi_{FD}$ was calculated from χ_{LF} and χ_{HF}, by:

$$\%\chi_{FD} = 100 * ((\chi_{LF} - \chi_{HF}) / \chi_{LF}).$$

The $\%\chi_{FD}$ is a measure of the amount of superparamagnetic magnetite particles (i.e < 0.03 μm) in the samples. This is often thought to be related to the amount of pedogenic enhancement in top soils with larger values for more pedogenic enhancement (Dearing et al. 1996). Values less than 4% are often typical of geological materials, although larger values are known from certain types of rock materials (Worm, 1998). Large $\%\chi_{FD}$ values may also be related to the residues from burning of archaeological materials (Peters et al., 2002).

Seven samples of material from representative features were collected to asses the variation of magnetic susceptibility with grain size (Table 3).These samples with an average weight of 0.5 kg were dried at room temperature and dry-sieved into seven grain size fractions: > 4 mm, 1.4-4 mm, 0.5-1.4 mm, 0.25-0.5 mm, 125-250 μm, 63-125 μu, and < 63 μm. Representative sub-samples of ~10 cm^3 from each fraction were placed in plastic pots and their χ_{LF} and χ_{HF} were measured.

4.2 Magnetic Remanence

All of the remanence directions and intensity values were measured using a Minispin spinner magnetometer housed in the Centre for Environmental Magnetism and Palaeomagnetism. Each of the plastic-box specimens were subjected to a program of measurement:

4.2.1 Initial (day 1) measurements

The natural remanent magnetisation (NRM) of each specimen was measured one day after their initial collection, which we have referred to as the NRM_1 value. The magnetic susceptibility was measured the same day. From these two measurements, the Koenigburger ratio (Q_N) was determined (Appendix 5). This is the ratio of the induced to remanent magnetisation of the samples. When Q_N values exceed 1, the remanence intensity is larger than the induced magnetisation of the specimen.

4.2.2 Assessment of viscous remanent magnetisation

After initial measurement all specimens were placed in a laboratory geomagnetic field of known orientation in such a position that the specimen was opposite in direction to the magnetic field at the Catholme site. This produces in the specimen a progressively larger new VRM in the new direction of the laboratory magnetic field, and the progressive loss of the VRM acquired by the specimen at the Catholme site (Appendix 1). Measurements of the new magnetic remanence acquired by the specimens were taken approximately 2, 4, 6, 8 and 12 weeks after initial collection. This observed build-up of VRM, for up to 3 months, allowed an estimate of the true intensity of the remanent magnetisation when the specimen was *in situ* (NRM_0). It also allowed an assessment of the longer-term VRM characteristics of the specimens. Through this process its possible to estimate the amount of VRM the specimens have lost between the time of collection and the time of first measurement (*i.e.*, one day later). See Appendix 1 for details.

4.2.3 Averaging the data

The data measured and determined from the measurements has a variety of distributions forms, from some data which is normally distributed to some which is log normally distributed, to some which is more bimodal in form. Hence, in order to maintain a consistency in reporting of this ‘average’ data, medians are determined as a measure of central tendency, and quartiles at 25% and 75% are reported (Q25/Q75), as a measure of the spread of the data about the central tendency.

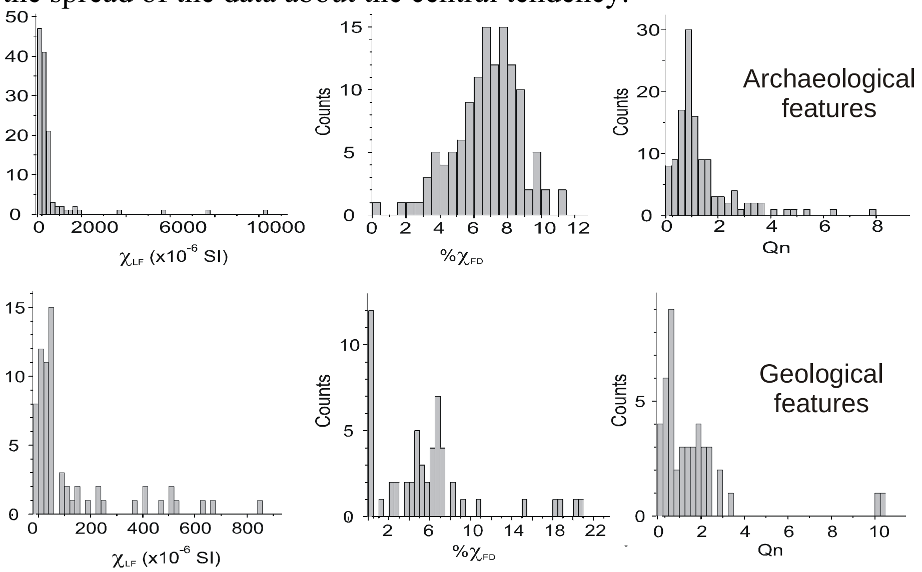

Figure 5. Examples of histograms for magnetic susceptibility, %χ_{FD} and Qnfor all specimens.

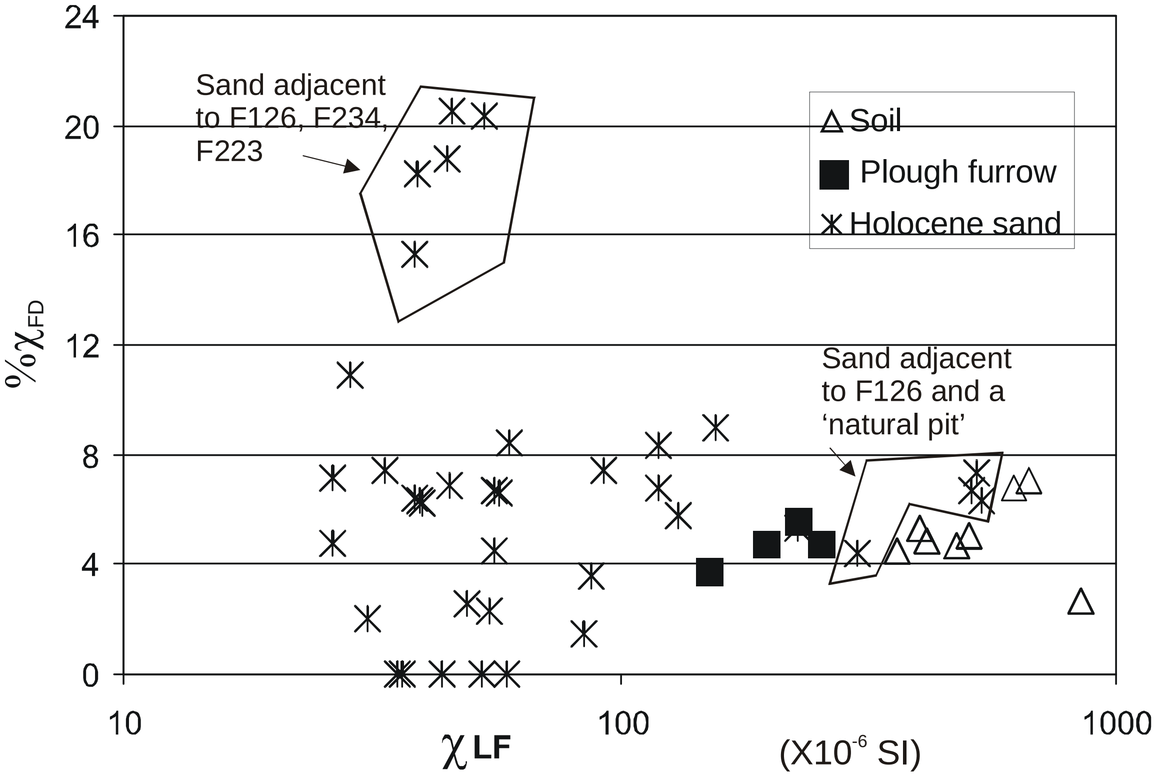

Figure 6 Magnetic susceptibility parameters for non archaeological materials on the Catholme site, excluding gravel clasts, which had $\%\chi_{FD}$ values below instrument sensitivity. Outlier samples from Holocene sand are indicated.

5 Results

5.1 Magnetic susceptibility

The magnetic susceptibility varies between very wide limits, from diamagnetic values of –1 x10^{-6} SI in the gravel clasts to about 10,000 x10^{-6} SI in some of the burnt features on the site (Figs. 6 & 7). Broadly the Holocene sands and gravel material have susceptibilities less than 100 x10^{-6} SI, the top-soils values around 500 x10^{-6} SI, and materials from plough furrows appear to be a mix of these two.

Surprisingly the $\%\chi_{FD}$ of the Holocene sands shows a large spread, from zero to about 20% (Fig. 6), overlapping with the tighter range shown by the soils (~5% on average). This can be explained by some contamination by the magnetic components from the archaeological fills perhaps in part due to water-induced infiltration of the fine-grained magnetic component in the soils/archaeological features into the sands. This is probably the case for all the specimens values with $\%\chi_{FD}$ values in excess of 12%, and some of the specimens with magnetic susceptibility in excess of 200 x10^{-6} SI (Fig. 6). Two specimens from a an interpreted 'natural pit' (B2-L19, L20), with magnetic susceptibility >300 x10^{-6} are probably an archaeological feature.

Most archaeological fills have magnetic susceptibility between 100 and 700 x10^{-6} SI, with only visibly burnt materials on the site have larger values (Fig. 7). The archaeological function classification produces broad groupings apparent in the $\%\chi_{FD}$ versus χ_{LF} relationships (Fig.7). The post-pits produce a grouping with somewhat lower χ_{LF} (<300 x10^{-6} SI), but larger $\%\chi_{FD}$ (>8%) than other fill materials. Huge pits, shallow pits and ring ditch materials fall within the range of $\%\chi_{FD}$ 6-9% and χ_{LF} 200-400 x10^{-6} same kind of values (Fig. 7). Linear ditch's and pit alignments typically produce lower χ_{LF} values (<200 x10^{-6} SI; Table 4).

Table 4. Median values of χ_{LF}, $\%\chi_{FD}$, Q_N, for every archaeological functional class and geological sample class. Values of $\%\chi_{FD}$ for gravel clasts were below instrument sensitivity, and Qn values for gravels are meaningless, since a sizeable proportion have diamagnetic (negative) susceptibilities. Particularly large median values are indicated by bold, and low median values in grey

		χ_{LF} (x10^{-6} SI)		$\%\chi_{FD}$		Q_N	
Feature classification	***N***	**Median**	**Q25/Q75**	**Median**	**Q25/Q75**	**Median**	**Q25/Q75**
Timber post pits	*18*	282	228/309	**8.2**	7.7/9.7	0.8	0.6/1.2
Pit alignments	*20*	61.2	38.2/176	4.9	3.1/5.4	1.6	1.3/1.8
Linear ditch	*10*	127	117/185	6.2	5.7/6.8	**2.5**	1.5/3.0
Ring ditch	*30*	199	7.8/317	7.3	5.7/8.0	0.8	0.7/1.1
Regular pits	*6*	84.9	63.2/261	4.9	3.7/5.9	**3.5**	1.5/3.6
Shallow pits	*6*	367	338/432	7.1	6.3/7.5	0.9	0.9/1.0
Huge pits	*18*	378	349/446	**8.6**	8.0/8.9	0.9	0.7/1.1
Burnt features	*12*	**1716**	1054/4167	6.8	6.4/7.1	0.6	0.4/1.7
Modern soil	*8*	**492**	411/633	4.9	4.6/5.6	0.6	0.4/0.8
Plough furrow	*4*	213	185/236	4.8	4.5/5.0	0.7	0.6/0.9
Holocene sands	*33*	53.9	39.1/91.5	6.5	3.8/7.4	1.4	0.6/2.1
Holocene gravel clasts	*20*	0.0	-1.30/3.3	—	—	—	—

Overall there appears to be 3 characteristic end-members in this $\%\chi_{FD}$ - χ_{LF} space.

- A source of burnt sand and silt materials with χ_{LF} >700 x10^{-6} SI, and $\%\chi_{FD}$ between 6-8% (Fig. 7).
- A 'post-pit' magnetic material which is shown by $\%\chi_{FD}$ often in excess of 8%.

A type of material exemplified by material from the pit-alignments. This could conceivable represent a mixture of sand-material, with a small amount of material typically from shallow or huge pits, since it strongly overlaps with the field typical of the Holocene sands.

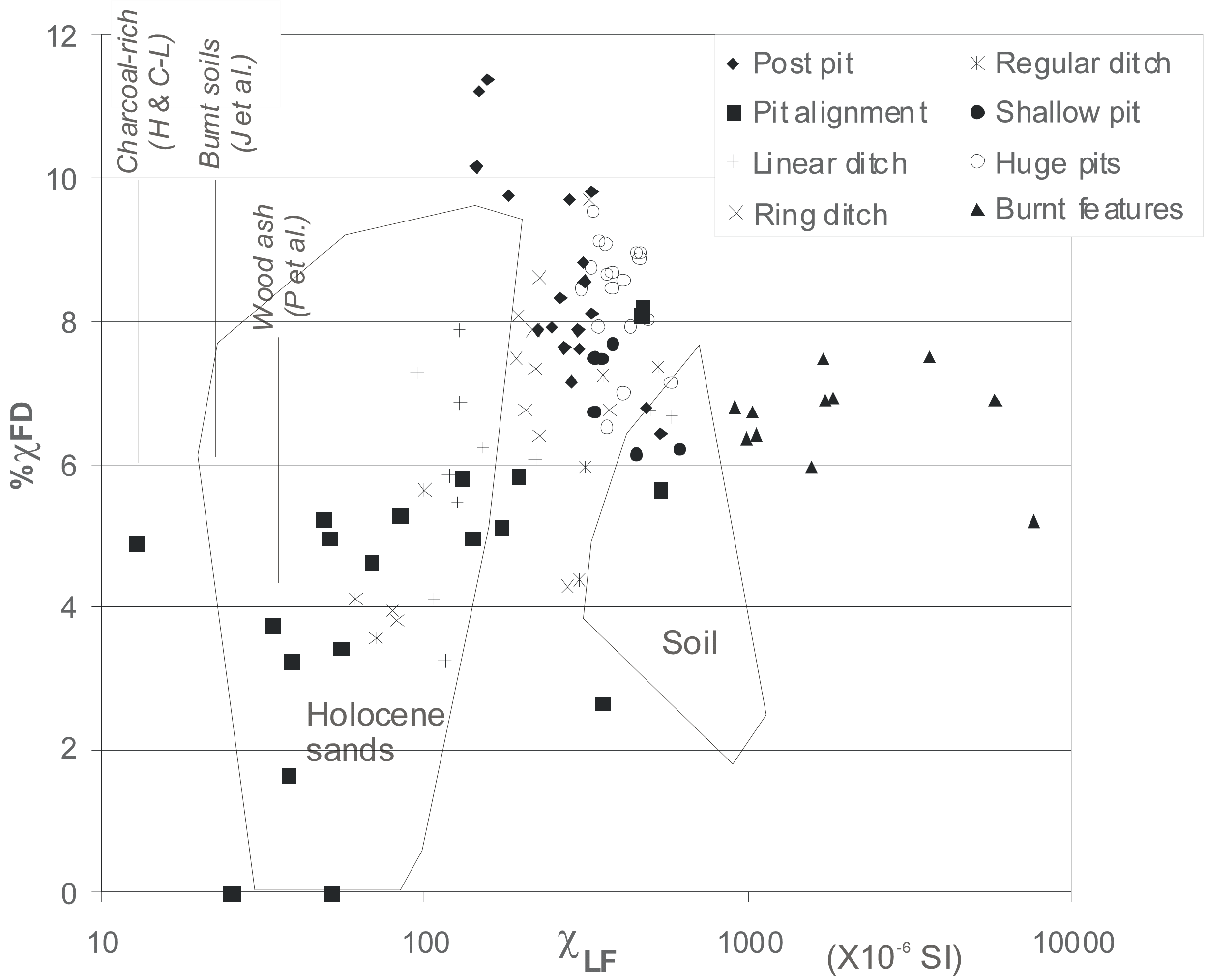

Figure 7 Archaeological materials and functions on the Catholme site. Fields which encompass the data for Holocene sands and soil from the Catholme site are indicated. Ranges of %χFD for burnt soils, wood ash and charcoal rich middens from Jordanova et al (2001) [J et al], Peters et al (2002) [P et al] and Hounslow and Chepstow Lusty (2002) [H &C-L].

The bulk of the archaeological fills fall within a %χ_{FD} - χ_{LF} space which cannot be generated by a mixture of Holocene sands and present-day top-soils. It seems likely that the source of this predominant magnetic material is burnt top-soil and fuel residues from burning. The %χ_{FD} values overlap with burnt-soils reported by Jordanova et al (2001) from various archaeological sites in Bulgaria, along with charcoal-rich midden material from a Roman bath house in Albania (Hounslow & Chepstow Lusty, 2002). The %χ_{FD} values are slightly larger than wood-derived ash reported by Peters et al (2002). The 'post-pit' magnetic material which is shown by %χ_{FD} in excess of 8% may be derived from the peculiar signal from *in situ* decay of wooden materials, giving rise to large amounts of very fine-grained ferrimagnetic particles. Alternatively it may relate to unusual sources of burnt material (cremations etc ?). The variability between archaeological functional classes suggests there was a profound difference in the material used for the filling of the various pit and ditch features. Is this related to age of these features or their functional purpose ??

The feature F126 in field B2 has by far the largest $\chi_{LF,}$ with a median value in excess of 1000 x10^{-6} SI (Table 5). This feature is associated with a large magnetic anomaly and burnt materials. Other relatively large χ_{LF} with median values >300 x10^{-6} SI are associated with various pit-features in fields A2 and B2 (Table 5). The two pit alignment features in field A1 (F211 and F212) have the lowest median χ_{LF} values with median values typically less than 50 x10^{-6} SI. These contrast with the other pit-alignment features in field A1, which have median values >150 x10^{-6} SI (Table 5). All the sampled features in field A2 have median *%χ_{FD}* greater than 7.4, which is distinct in comparison to samples from other fields, which have values mostly less than this. This may indicate a unusual superparamagnetic particle generation process, specific to this field.

Table 5. *Average values of χ_{LF}, %χ_{FD}, Q_N, for features sampled for magnetic property analysis. Particularly large median values are indicated by bold, and low median values in grey.*

Field. Feature	Class	N	χ_{LF} (x10^{-6} SI)		%χ_{FD}		Qn	
			Median	Q25/ Q75	Median	Q25/ Q75	Median	Q25/ Q75
A1. F211	Pit alignment	6	50.6	48.4/53.7	4.4	3.5/5.2	1.4	1.1/1.6
A1. F212	Pit alignment	7	37.8	24.9/53.1	3.3	0.8/4.8	1.6	1.1/2.5
A1. F217	Pit alignment?	3	471	467/501	**8.1**	6.9/8.2	1.6	1.5/2.1
A1. F218	Pit alignment	4	182	149/233	5.2	4.5/5.4	1.6	1.4/1.8
A1.Mag±	Mag. anomaly	3	45.3	44.6/47.1	2.6	1.3/4/7	**10.1**	6.7/10
A2. F221	Post-pit	4	254	240/265	**7.9**	7.8/8.0	0.8	0.7/0.8
A2. F223	Huge pit	18	**378**	349/446	**8.6**	8.0/8.9	0.9	0.7/1.1
A2. F234	Post pit	6	169	149/258	**10.0**	8.1/11.0	0.6	0.2/1.1
A2. F241	Shallow pit	4	**367**	347/399	**7.5**	7.1/7.5	0.9	0.8/1.0
B2. F105.08	Ring ditch	4	274	222/335	**7.3**	6.7/8.3	0.8	0.7/0.8
B2. F105.10	Ring ditch	13	188	51.3/482	**7.7**	6.1/8.0	0.9	0.8/1.6
B2. F105.11	Ring ditch	4	162	111/228	6.5	5.5/7.4	1.1	1.0/1.4
B2. F118	Shallow pit	2	**474**	404/545	6.5	5.5/7.4	1.1	1.0/1.4
B2. F126	Regular pit (burnt)	12	**1716**	1054/4167	6.8	6.4/7.1	0.6	0.4/1.7
B2. F134	Post pit	2	**507**	494/521	6.6	6.5/6.7	1.1	1.0/1.1
B2. F141	Regular pit	2	**334**	325/344	6.6	6.3/6.9	0.8	0.8/0.9
F1. F315	Linear ditch	6	122	116/128	6.5	5.9/7.2	**3.0**	2.8/3.2
F1. F317	Linear ditch	5	219	126/495	6.1	5.5/6.7	1.4	1.1/1.6
F1. F320	Ring ditch	5	192	82.1/193	**7.5**	4.6/8.1	0.2	0.2/0.6
F1. F321	Regular pit	4	65.6	60.1/77.6	3.8	2.4/4.5	**3.6**	3.6/4.7
F1. F324	Ring ditch	4	211	173/233	5.5	4.2/6.9	0.9	0.7/2.0

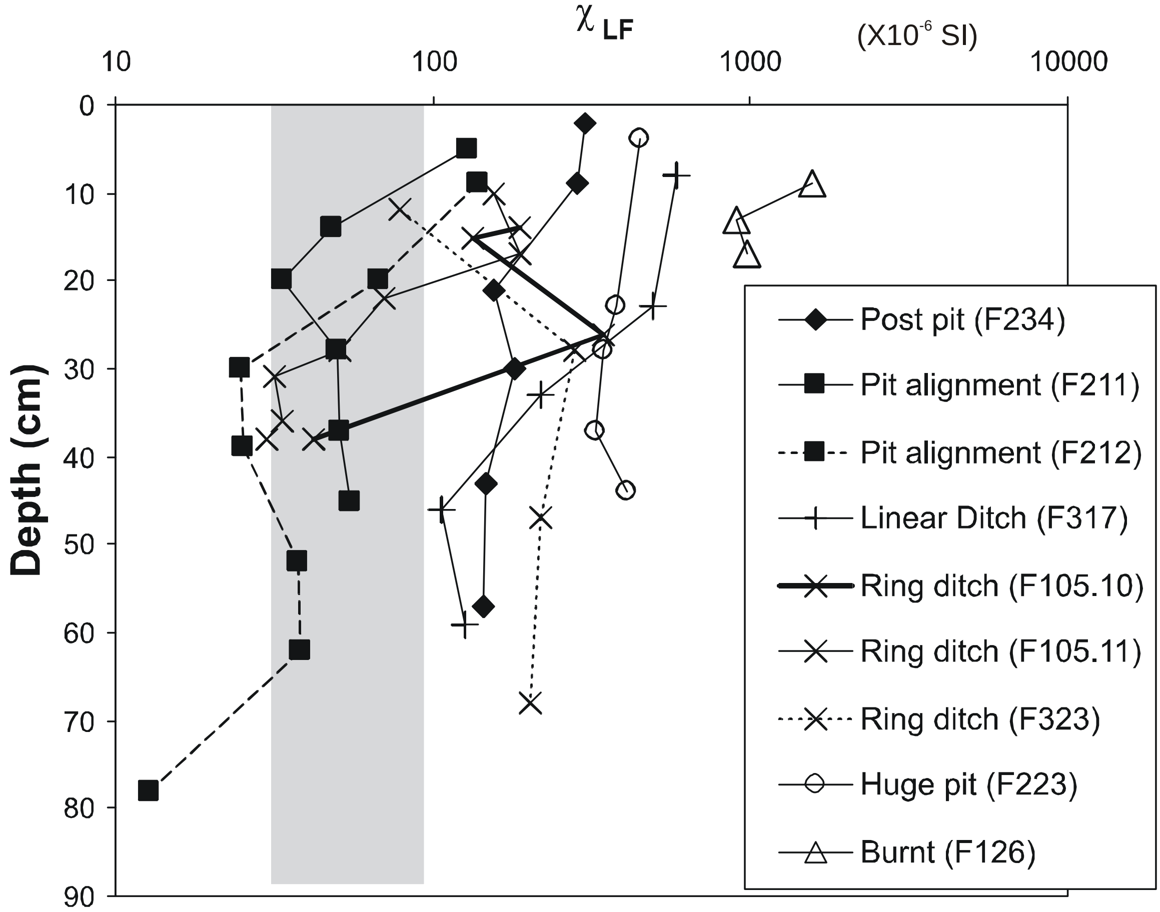

Fig. 8. Magnetic susceptibility variation with depth, for all the depth profiles from various features. The 25 to 75% quartile range for the Holocene sands is indicated in the grey bar.

Generally the magnetic susceptibility varies significantly with depth within the various types of features sampled. Of the 9 features sampled with depth, 6 of these have the largest magnetic susceptibility in the uppermost specimen. The other three features are ring ditch features which have more variable magnetic susceptibility with depth (Fig. 8).

5.1.1 Magnetic susceptibility variation with grain particle size

Overall the grain size fractions do not show large differences between the various fractions. The expectation was that the finest fraction (<0.063 mm) would have by far the largest magnetic susceptibility. This is the case in 5 out of the 7 samples, the two exceptions being the samples from pit alignment and ring ditchs. All samples appear to show a decline in the magnetic susceptibility from the finest fraction up to the 0.250 mm fraction, which is followed by a peak in the 0.5 or 1.4 mm fractions (Fig. 9). The $\%\chi_{FD}$ does not show this bi-modal behaviour to the same extent, indicating that this property is not unexpectedly predominantly located in the finer-fractions.

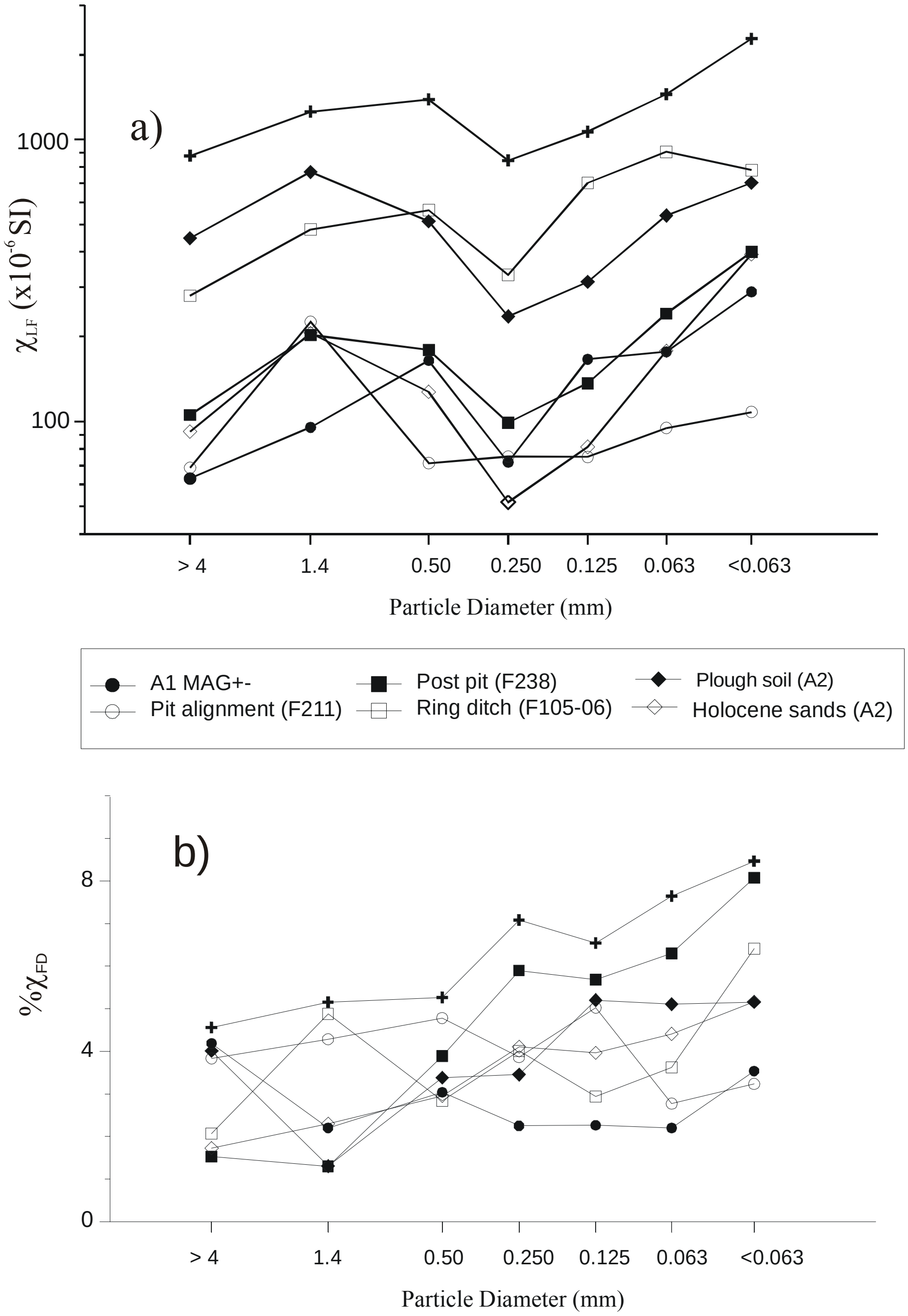

Fig. 9. Variation of magnetic susceptibility and %χ_{FD} with particle size for samples representative of the various types of functional features at Catholme.

5.1.2 Cross calibration of in situ and laboratory χ_{LF}

The set of 27 samples whose magnetic susceptibility χ_{LF} had been previously measured *in situ* at the site using the MS2F probe by Meg Watters were re-measured in the laboratory. As the samples bags contained a varying amount of material between 2 and 12 grams, the laboratory mass specific magnetic susceptibility values were re-calculated to volume specific values, using the average bulk density of 13 samples (Fig. 10). The resolution of the field measurements is some 1 order of magnitude less sensitive than the laboratory measurements, which has contributed to the large scatter in the cross plot (Fig. 10). Overall the *in situ* measurements are some 48% of the laboratory measurements. This is close to the 50% value quoted in the Bartington Instruments manual for the MS2F probe. This difference may not be significant considering the scatter in the data.

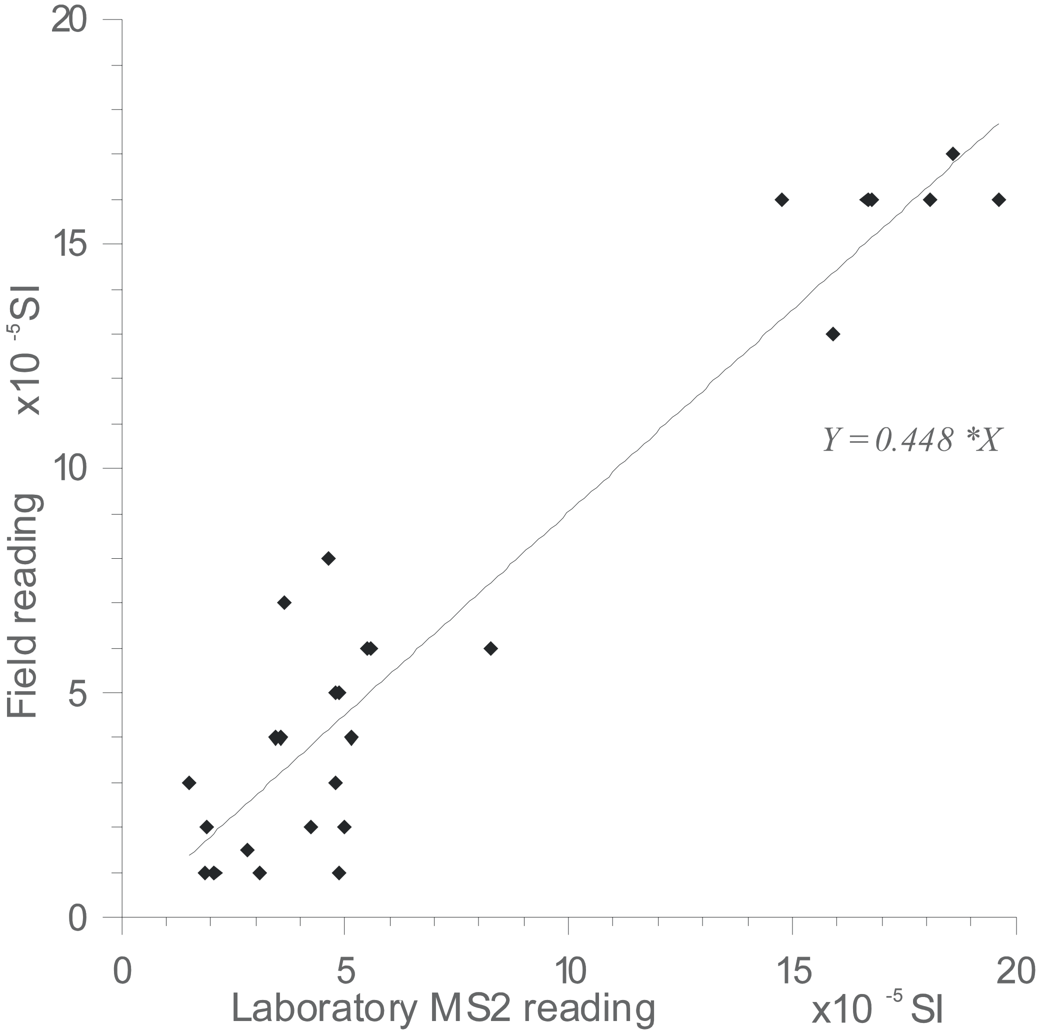

Fig. 10. Comparison of the in-situ and laboratory-measured sub-samples of magnetic susceptibility (χ_{LF}) on a set of 27 samples.

5.2 The NRM directions and intensity

The NRM_1 intensities of the non-archaeological materials are <2 mA/m in the gravel clasts and upto about 10 mA/m in the Holocene sands (Fig. 11; Table 6). The mid to upper range of NRM_1 values for the Holocene sands overlap with the lower range typically found in the modern top-soils and material from the plough furrows. The median Qn values of the Holocene sands are greater than 1 whereas the soil and furrow material generally have Qn <1 (Fig. 11; Table 4).

The material from archaeological fills shows a wide range of NRM_1 intensities from a lower range of ~1mA/m to values of about 20 mA/m (Fig. 12). The NRM_1 intensities are not strongly related to the archaeological functional groupings although material from ring ditchs and pit alignments commonly range into values <10 mA/m (Fig. 11). The specimens from pit alignments, linear ditches and regular pits have median Qn >1, whereas huge pits and ring ditches have median Qn <1. This same group of functional features also have relatively small χ_{LF} values (typically < 200 x10^{-6} SI), and median

$\%\chi_{FD}$ <6.3 (Table 4). This reflects a difference in magnetic mineral properties.

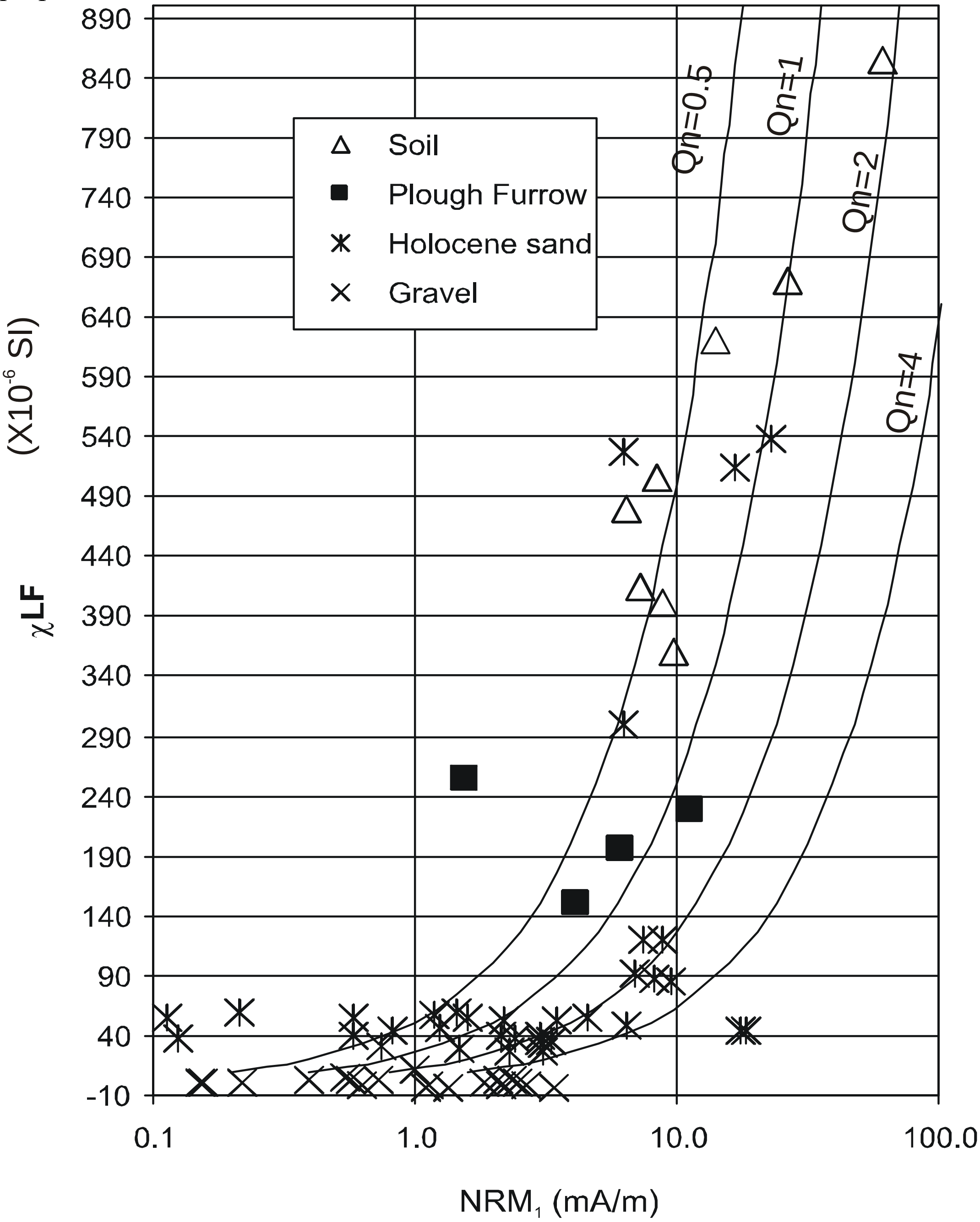

Figure 11. Variation of NRM_1 with magnetic susceptibility for non-archaeological materials.

Table 6. Median NRM intensities of the functional classes. M=magnitude of vectorial mean, R=unit vector dispersion from Fisher mean direction calculation, (D,I)= vectorial mean declination, inclination (i.e not Fisher mean). Q25/Q75 are quartile 25% and 75% values. Medians, Q25/Q75, M in units of mA/m. Particularly large median values are indicated by bold, and low median values in grey.

Feature class	***N***	**NRM_1 (mA/m)**		**Vectorial mean**		**NRM_0 (mA/m)**	
		Median	**Q25/Q75**	**M**	**R (D,I)**	**Median**	**Q25/Q75**
Timber post pits	*18*	8.6	6.5/15	8.2	0.83 (5,61)	12.6	9.8/21
Pit alignment	*20*	3.6	2.4/11	8.1	0.71 (342,63)	5.4	3.5/12
Linear ditch	*11*	**14.3**	12.717	**15.0**	0.98 (358,72)	16.3	14/18
Ring ditch	*30*	6.5	2.5/12	9.0	0.88 (347,65)	9.8	3.7/17
Regular pits	*6*	11.1	10/13	11.9	0.98 (342,67)	15.5	13/16
Shallow pits	*6*	12.6	12/16	**15.4**	0.98 (342,58)	**18.3**	17/22
Huge pits	*17*	13.3	11/17	13.6	0.92 (346,71)	**18.1**	14/23
Burnt feature	*11*	**38.5**	26/291	**401**	0.69 (359,42)	**37.9**	22/86
Top-Soil	*8*	9.3	8.1/17	8.1	0.65 (328,79)	16.4	9.9/26
Plough Furrow	*4*	5.2	3.5/7.5	5.7	0.97 (354,51)	6.8	5.4/8.7
Holocene sands	*35*	3.0	1.4/6.7	4.0	0.79 (307,68)	4.6	2.1/9.6
Gravels	*20*	1.10	0.50/2.1	0.71	0.33 (272,-27)	__	__

Burnt features on the site which in our sampling are associated with regular pits in field B2 (feature F126), mostly have NRM_1 intensity similar to the upper range of values found in other archaeological fills (Fig. 13). This is accept for 3 specimens, at the gravel surface of feature F126, which show an order of magnitude larger NRM_1 intensity. These three specimens largely represent the product of an *in situ* TRM, although the NRM_1 directions of these 3 specimens are not along the present-day field direction, indicating some tilting, since their last heating.

Like the magnetic susceptibility, the NRM_1 intensity values vary strongly with depth, with the largest values generally from the upper-most samples near to the sub-soil level.

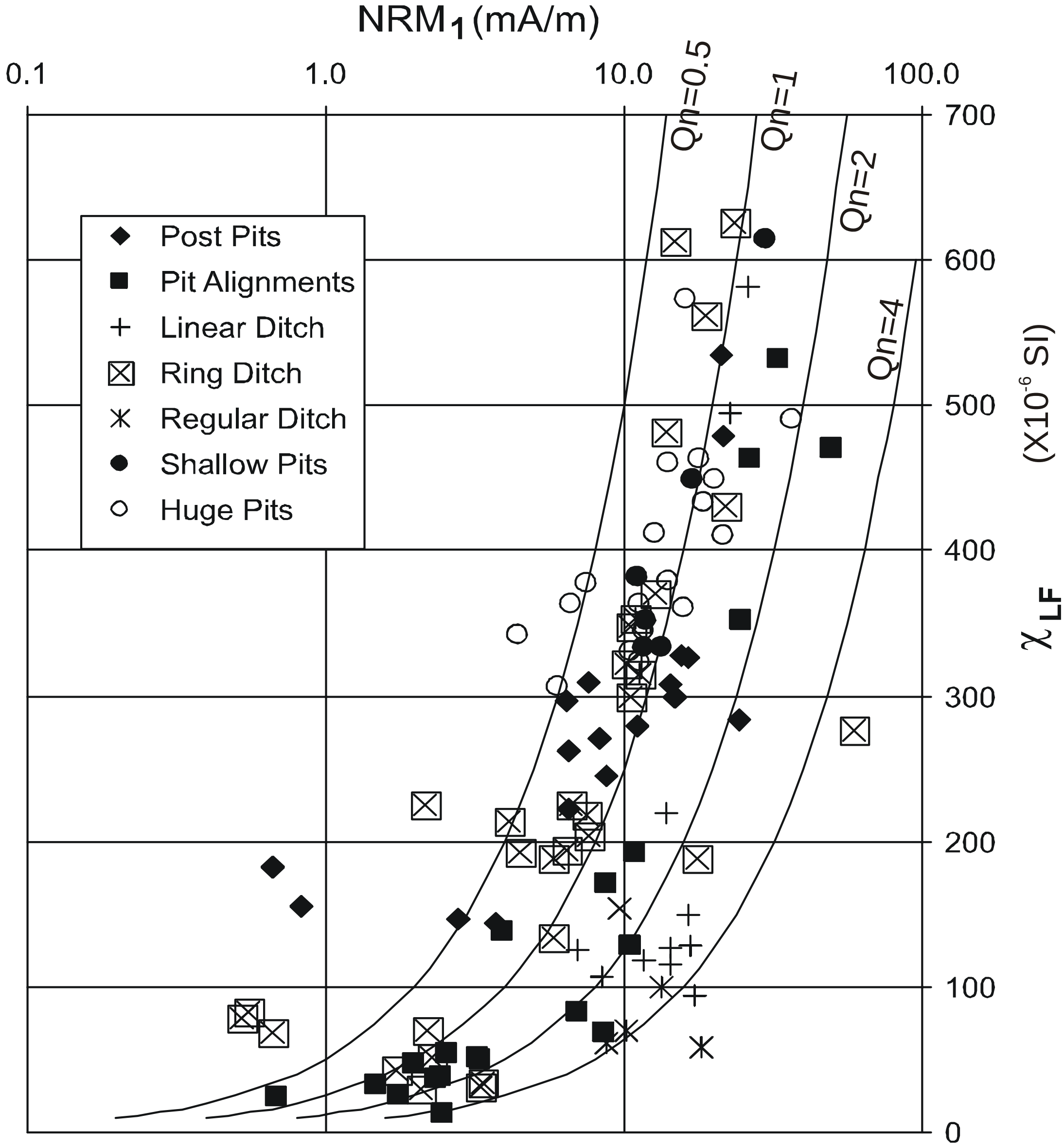

Figure 12 Variation of NRM$_1$ with magnetic susceptibility for archaeological materials

The specimens not from archaeological materials display a large scatter in their NRM$_1$ directions (α_{95} = 15.8$^{o;}$ Fig. 14b). Their mean direction (D = 329^o, I = 60.8^o) deviates strongly from the local magnetic field at the site. This is especially so for the gravel clasts which are highly scattered in direction (Fig A1.10). This indicates that the gravel clasts retain a stable remanent magnetisation from their original orientation in their host rock mass, and are not strongly affected by acquisition of VRM at Catholme. This is born out by the VRM determinations (Appendix 1). If there is a sizeable proportion of rock fragments as sand-sized or larger clasts in the Holocene sand deposits, then it is likely that this contributes to the scatter in NRM$_1$ directions evident from the Holocene sand specimens.

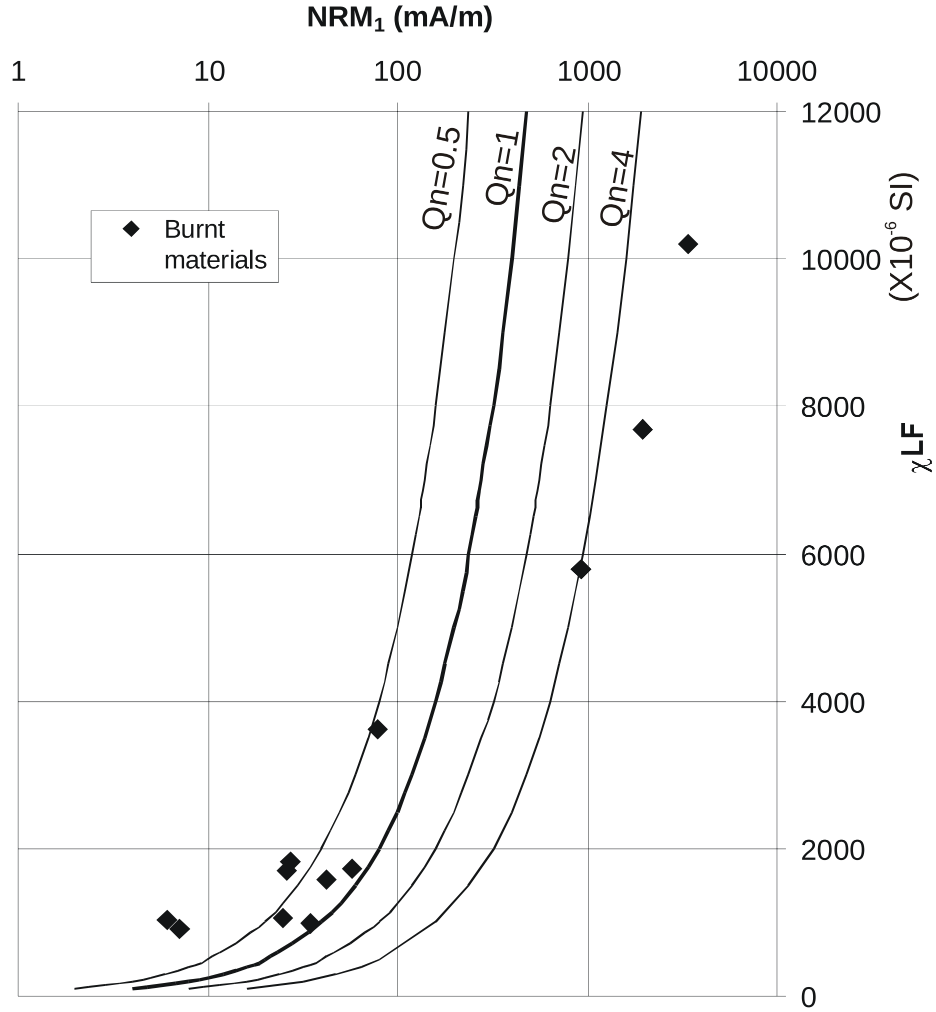

Figure 13. Variation of NRM_1 with magnetic susceptibility for burnt materials

The mean NRM_1 direction of specimens from archaeological fills is $D_{mean} = 357.8^o$, $I_{mean} = 69.5^o$, $\alpha_{95} = 5.5^o$ (Fig. 14a). This is statistically the same as the local magnetic field from the site using the IGRF model (*e.g.*, $D = 356.2^o$, $I = 67.4^o$ Nasa, 2004). The scatter evident in the specimen directions in Fig. 14a could be due to VRM acquisition since the time of collection or due to sample disturbance whilst collection, or natural directional variability (see Appendix 1 for details).

The average remanent magnetisation of the materials at any one location on the Catholme site will be the vectorial mean of the *in situ* remanent magnetisation vectors, rather than the median as used in Table 6. This vectorial average is more strongly influenced by those materials which show the larger remanence magnitude. This is demonstrated by the vectorial mean of the NRM_1 directions shown in Table 6. Hence this produces larger vectorial magnitudes (M) of the remanence directions, than those given by the medians. This is particularly noticeable for pit alignment and burnt features which are some 2 and 10 times larger than their medians (Table 6). These two types of features also have a larger direction dispersion in the vectorial mean evident by the smaller R value (Table 6). For other feature classes medians seem to reproduce the a magnitude similar to the vectorial mean (Table 6).

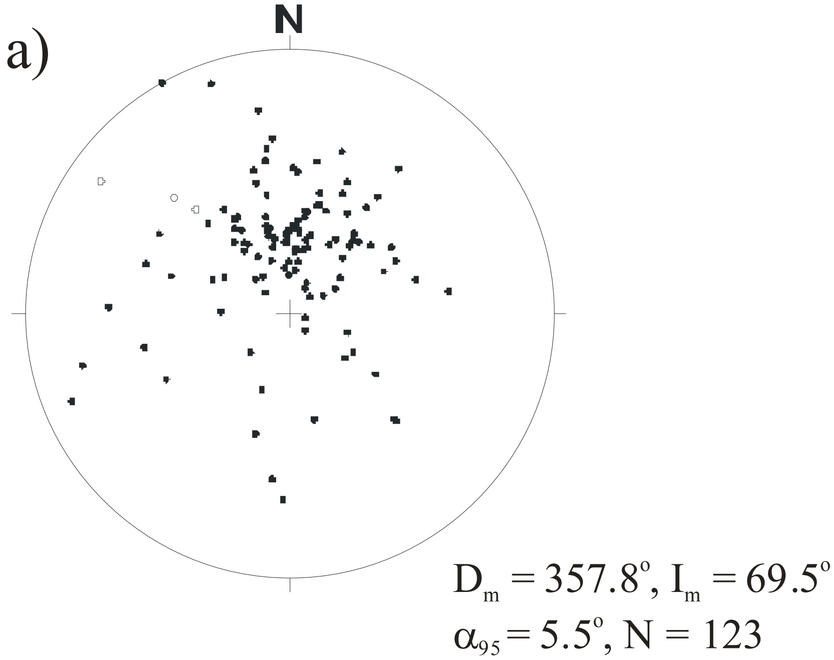

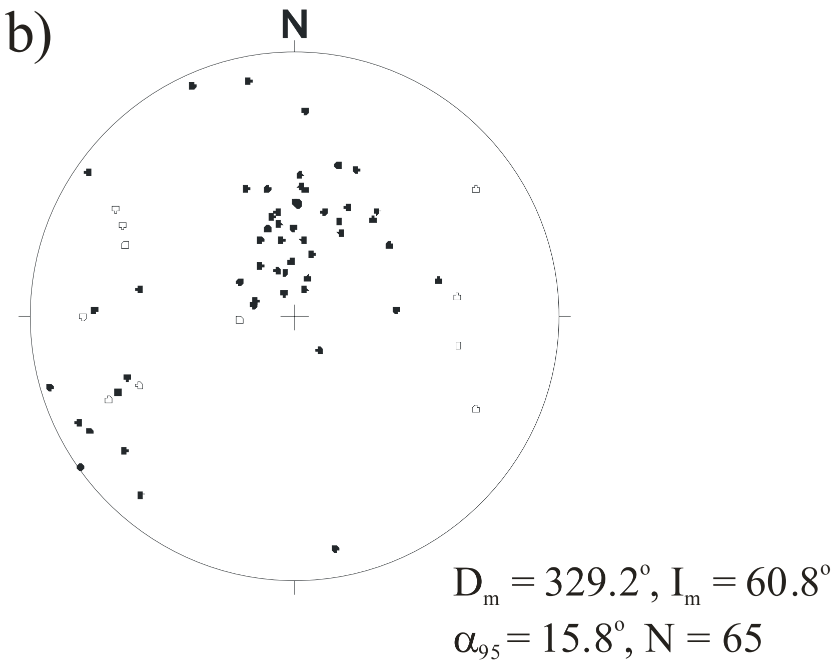

Figure 14. Stereoplots of the NRM directions in a) the archaeological features, and b) in other features.

5.3 Magnetic viscosity and the *in situ* remanence intensity (NRM_0)

Three values express the magnetic viscosity behaviour of these specimens:

- **S**: which is the amount of long-term VRM acquired, expressed over one interval of log time. This is discussed further in Appendix 1.
- **VRM_1**: which is the amount of remanence apparently lost between the sampling, and first remanence measurement (on day 1). This is estimated by the VRM lost between day 1 and about day 15 (Appendix 1). The relative importance of VRM

loss up to the first measurement on day 1 can be gauged by the ratio (as a percentage) of the VRM_1/NRM_1 (Table 7).

- **VRM_T**: which is an estimate of the amount of VRM acquired by the specimen, since antiquity and the day 1 measurement. This is determined by laboratory remanence measurements up to 3 months after sample collection (Appendix 1), and is also listed in Table 7.

VRM_T (and VRM_1) was negligible (< 1 %) in the gravel clasts, being below the accuracy of the measurements (see appendix 1 for details). This combined with the gravels' weak but very scattered NRM_1 directions indicates that their contribution to the total remanent magnetisation of large volumes of material (~1-10 m^3) at the site will be minimal, since their vectorial means will be near zero.

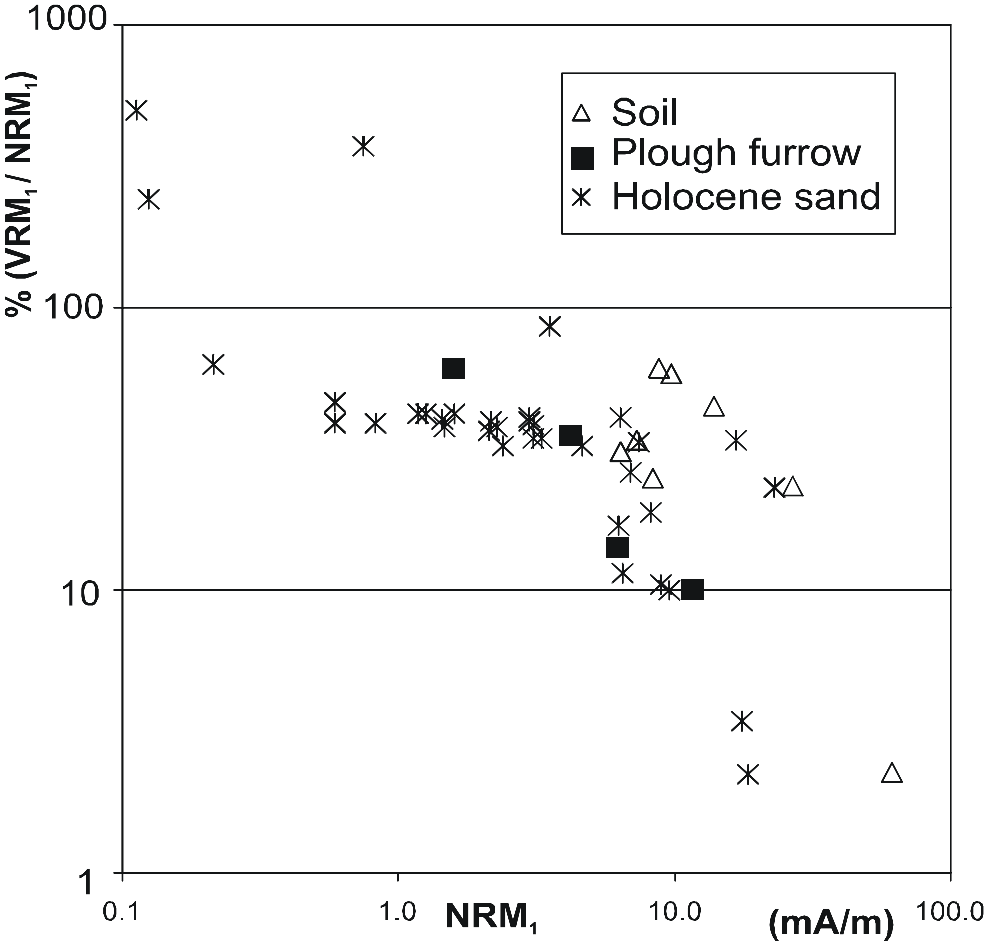

Figure 15. The percentage of VRM lost (VRM_1) expressed as a proportion of the NRM_1 magnitude, for non-archaeological samples from the site.

In the non-archaeological materials there is an approximate inverse relationship between NRM_1 and $\%VRM_1/NRM_1$ (Fig. 15). In these materials most specimens with NRM_1 intensities of 1 to 10 mA/m have NRM_0 values which should be some 125% to 140% larger than the NRM_1 values ($\%VRM_1/NRM_1$ of 25 to 38%; Table 7; Fig. 15). This drops to mostly <120% for materials with NRM_1 intensities greater than 10 mA/m.

For the archaeological fills, the lowest median values of $\%VRM_1/NRM_1$ are for the burnt features and linear ditch materials (from field F1), with NRM_0 values < 120% of NRM_1 (Table 7). Fills with high median values of $\%VRM_1/NRM_1$ greater than 45% are displayed by pit alignment, post pit and shallow pit features (Fig. 16; Table 7). Other types of features (ring ditch, regular pit and huge pit) display intermediate values (Fig. 7).

Table 7. Median VRM intensities of the functional classes. Q25/Q75 are quartile 25% and 75% values. Medians, Q25/Q75. Particularly large median values are indicated by bold, and low median values in grey.

Feature class	***N***	**VRM_1 (mA/m)**	**% VRM_1/ NRM_1**	**VRM_T (mA/m)**	
		Median	**Median**	**Median**	**Q25/Q75**
Timber post pits	*18*	3.79	**46**	11.7	8.7/17
Pit alignment	*20*	1.44	**57**	3.4	2.6/11
Linear ditch	*11*	1.7	13	10.1	4.7/15
Ring ditch	*30*	2.22	43	7.5	3.9/16
Regular pits	*6*	2.45	26	7.5	4.9/10
Shallow pits	*6*	5.85	**46**	18.1	17/22
Huge pits	*17*	3.86	39	14.3	12/24
Burnt feature	*11*	5.60	19	17.9	8.2/42
Top-Soil	*8*	3.92	33	16.8	15/18
Plough Furrow	*4*	1.06	25	15.7	14/18
Holocene sands	*35*	0.86	38	3.0	2.0/6.2
Gravels	*20*	—	—	—	—

The contribution of VRM_T to NRM_0 is about 70% in the Holocene sands. The other 30 % of the NRM_0 signal reflects the specimen disturbance during collection, as well as the errors in estimating the true NRM of the feature due to the small sampling volume (8 cm^3). The specimens also occasionally contain a number of randomly oriented pebbles and smaller rock fragments, whose randomly oriented remanent magnetisation will not be averaged and will contribute to the total NRM because of the small sample volume. Overall in the archaeological materials the VRM_T accounted for on average 91 % of the measured NRM_0 intensity. The VRM_T is an upper limit for the estimated VRM acquired by the specimens, since its calculation does not account for any other *in situ* magnetisation processes that may contribute to the NRM (see Appendix 1).

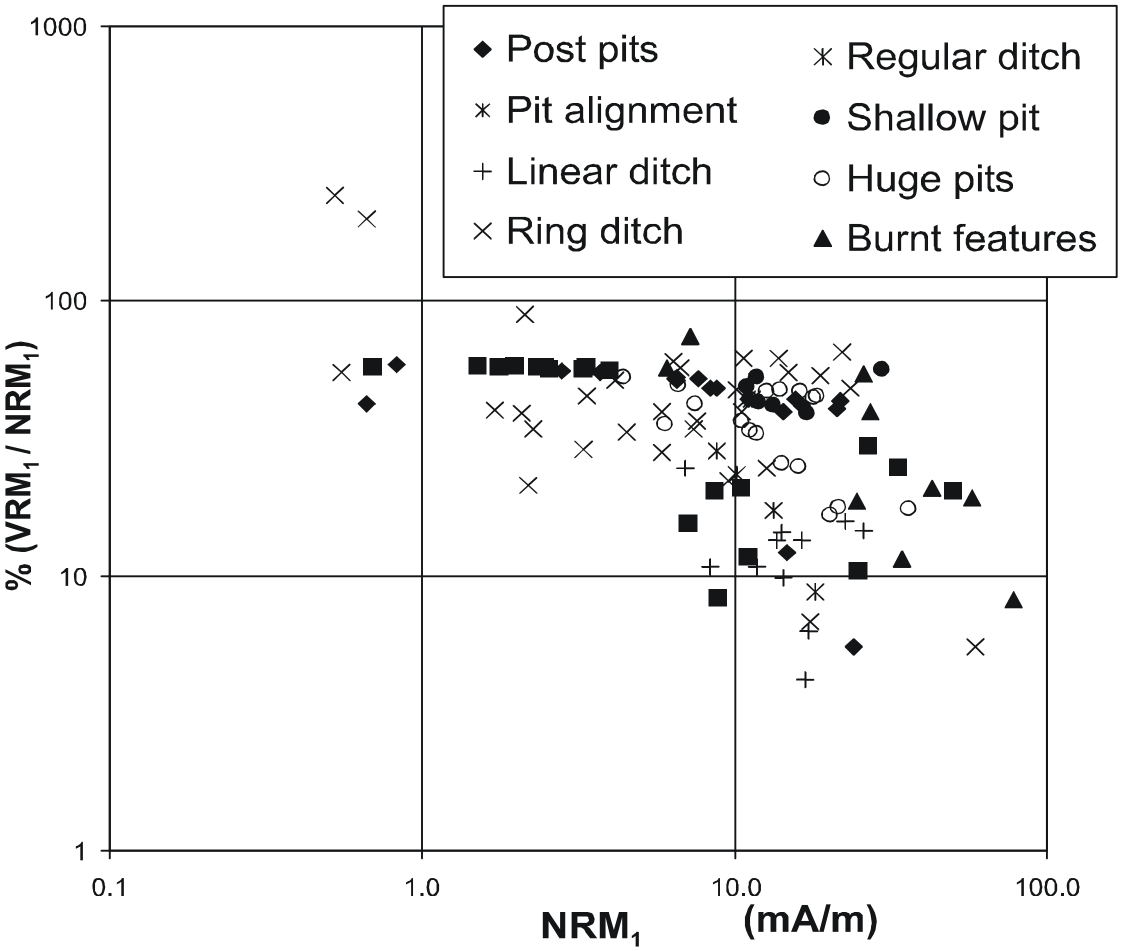

Figure 16. The percentage of VRM lost (VRM_1) expressed as a proportion of the NRM_1 magnitude, for the various classes of archaeological feature from the site.

6 Discussion

There are several issues which related to the significance of this magnetic data to the Catholme site, in terms of the aims as set out originally.

6.1 How representative is this data for Catholme site ?

In a sense every feature on the site is a singularly unique, since the reasons for the physical characteristics of the archaeological fills could conceivably be slightly different from adjacent features which originally served the same function. The variability of magnetic properties within a single archaeological functional class is quite large, certainly comparable to the variability between functional classes (Fig 17).

As a result of the strong depth-related changes in the magnetic susceptibility and NRM_1 intensity, it is probable that the true variability in magnetic properties is underrepresented in the data, because some types of features are overrepresented by data from horizontal traverses near the top of the archaeological features or at the sub-soil level (e.g. regular and shallow pits). Such sampling will bias the average data to larger values because of the general down-wards decrease in magnetic susceptibility and NRM intensity. Hence, as well as average values for the functional classes throughout their volume, some idea of the average depth variation with different types of functional classes would be helpful in understanding the 3-D variation in magnetisation intensity, and its affect on the magnetic anomalies. This has probably not been adequately achieved with the existing limited dataset.

Table 8. NRM and VRM intensities of the sampled archaeological features. Q25/Q75 are quartile 25% and 75% values. Particularly large median values are indicated by bold, and low median values in grey.

Field. Feature	**Class**		**NRM_1 (mA/m)**		**NRM_0 (mA/m)**		**VRM_T (mA/m)**	
		N	**Median**	**Q25/ Q75**	**Median**	**Q25/ Q75**	**Median**	**Q25/ Q75**
A1. F211	Pit alignment	6	2.9	2.1/3.3	3.8	3.2/4.6	3.0	2.2/3.5
A1. F212	Pit alignment	7	2.4	2.0/3.2	3.6	2.7/4.9	2.5	1.3/2.6
A1. F217	Pit alignment?	3	**33.0**	30/41	**40.0**	37/49	**46.3**	45/48
A1. F218	Pit alignment	4	9.9	8.3/14	10.8	9.1/16	12.8	8.9/17
A1.Mag±	Mag. anomaly	3	17.7	12/18	17.7	12/18	9.6	5.9/10
A2. F221	Post-pit	4	7.4	6.5/8.4	11.1	9.9/12	8.1	7.7/8.8
A2. F223	Huge pit	18	13.3	11/17	18.1	14.2/23	13.5	12/24
A2. F234	Post pit	6	3.3	1.3/12	5.0	2.0/13	10.7	9.4/15
A2. F241	Shallow pit	4	12.6	12/14	17.8	17/20	18.1	17/20
B2. F105.08	Ring ditch	4	8.4	6.0/11	12.6	9.3/15	12.0	6.2/18
B2. F105.10	Ring ditch	13	9.6	3.3/15	11.3	4.2/23	7.1	3.1/17
B2. F105.11	Ring ditch	4	8.2	4.8/12	10.9	6.0/16	8.0	4.5/12
B2. F118	Shallow pit	2	20.7	16/25	31.8	25/39	23.8	18/29
B2. F126	Regular pit (burnt)	12	**38.5**	26/291	**38.3**	30/102	**86.1**	44/90
B2. F134	Post pit	2	21.5	21/22	30.1	30/31	18.6	18.2/19
B2. F141	Regular pit	2	11.1	11/11	15.8	16/16	10.1	10/10
F1. F315	Linear ditch	6	15.3	14/17	16.9	16/18	11.9	6.7/16
F1. F317	Linear ditch	5	13.7	8.4/23	15.4	9.3/25	9.5	3.8/10
F1. F320	Ring ditch	5	2.1	0.7/4.5	3.6	2.0/6.0	3.9	3.1/7.9
F1. F321	Regular pit	4	11.7	9.9/15	14.1	12/17	5.0	4.8/8.7
F1. F324	Ring ditch	4	7.5	5.7/20	9.8	7.6/23	10.1	5.5/15

The data when converted to NRM_0 intensities clearly shows the importance of the *in situ* remanent magnetisation for determining the total magnetisation intensity (Fig. 17). This is particularly for pit alignment, regular pits and linear ditches which have median Qn values greater than 2, indicating the induced magnetisation (i.e. due to magnetic susceptibility) contributes less than $1/3^{rd}$ of the net magnetisation. It is predominantly only for burnt features that the induced magnetisation dominates (Qn <1; Fig. 17)

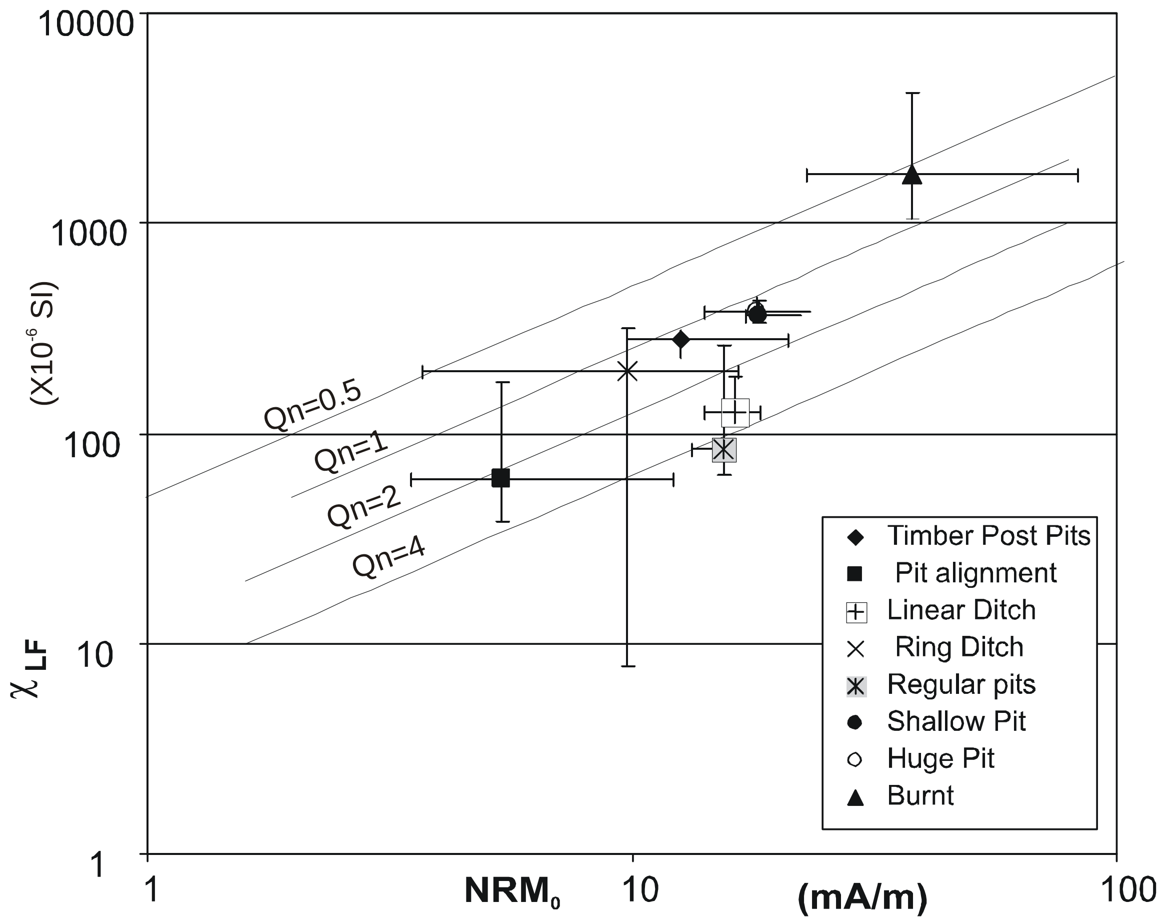

Figure 17. Median values of χLF and NRM_0 values for each functional class. The error bars represent the 25% and 75% quartile values, indicating that 50% of the data fall within this window. The lines of equal Qn are based on NRM0, the estimated in situ remanent magnetisation.

6.2 Is this data consistent with the observed magnetic anomalies?

If the magnetic property data is a good representation of typical features, on the site, then forward modelling of magnetic anomalies should approximately match the actual measured anomalies. This forward modelling was attempted using sampled features from the site (Table 9).

Simple modelling was done using two types of models, which predict the vertical magnetisation component produced by a body with a net magnetisation contrast.

- A single dipole model which approximates to a buried sphere of material. We used this as an approximation for pit-type features, with a depth of the dipole at ½ the maximum depth of the feature.
- Line of dipoles, which approximates to a buried cylinder of material. We used this approximation for ring and linear ditch type features, with dipole depth at ½ the depth of the ditch feature, and cross sectional area of the cylinder equivalent to the cross sectional area of the ditch.

Field	Feature (anomaly position)	Magnetometer/ survey level	Measured Anomaly: Mean anomaly (nT)	Error on mean (nT)	Calculated anomaly (nT)	Model
A2	F221	G858/soil	5.56	0.50	0.99	Sphere
A2	F241	G858/soil	3.17	0.35	0.09	Sphere
A2	F234	G858/soil	6.69	2.01	0.28	Sphere
A2	F223 (East)	G858/soil	7.15	1.00	1.29	Cylinder
A2	F223 (West)	G858/soil	2.81	0.50	1.29	Cylinder
B2	F126	G858/soil	14.81	0.36	13.19	Cylinder
B2	F105.11	G858/soil	4.31	0.22	1.92	Cylinder
F1	F315	G858/gravel	4.55	0.30	4.72	Cylinder
B2	F118	G858/gravel	1.43	0.06	4.22	Sphere
B2	F134	G858/gravel	1.18	0.11	4.33	Sphere
F1	F321	G858/gravel	3.55	0.59	5.99	Sphere
A1	F217	G858 gravel	9.60	0.20	3.79	Sphere
A1	F218 (west flank)	G858 gravel	1.99	0.49	10.13	Sphere
A1	F212	G858 gravel	1.88	0.43	-0.01	Sphere
F1	F317	G858/gravel	9.27	0.61	7.28	Sphere
B2	F126	G858/gravel	17.89	0.22	45.11	Cylinder
F1	F324	G858/gravel	2.10	0.18	4.54	Cylinder
F1	F320	G858/gravel	3.86	0.13	2.39	Cylinder
B2	F105.11	G858/gravel	3.66	0.35	6.10	Cylinder
B2	F105.11	G858/gravel	1.60	0.11	3.61	Cylinder
B2	F141	FM256/gravel	1.97	0.40	39.20	Sphere
F1	F315	FM256/gravel	2.33	0.29	3.95	Cylinder
B2	F105.08 (North)	FM256/gravel	7.41	0.65	8.54	Cylinder
B2	F126	FM256/gravel	53.39	4.40	96.69	Cylinder
B2	F105.10	FM256/gravel	5.09	0.65	8.54	Cylinder

Table 9. Magnetic gradient anomalies and their equivalent calculated anomalies. Soil thickness used in field F1=0.5m, in other fields, 0.4m. For G858, lower sensor at 0.3m, upper at 1.3m; for FM256, lower sensor at 0.3m, upper at 0.8m. Measured anomalies typically comprised 3-4 readings from peak and 3-4 from trough or background.

Both of these simple models are outlined in Sharma (1997), or most other standard geophysical texts. For each of the features in Table 9 the median magnetic susceptibility and NRM_0 was determined. This was used in combination with the median magnetic susceptibility and NRM_0 of the Holocene sands to determine the net induced + remanent magnetisation contrast between the underlying geology and the archaeological feature. This necessitated the determination of the volume of the archaeological feature for the dipole model (see appendix 4 for details). The cross sectional area of the feature was sufficient for the line of dipoles model (Appendix 4). We calculated the magnetisation produced at both the upper and lower sensor positions for both the G858 and FM256 gradiometers. From these two values we could determine the vertical magnetic field gradient. We did these model calculations using the 25% quartile, median and 75% quartile values for the various archaeological features, to give the likely range in calculated anomaly.

The magnitude of the magnetic anomalies was extracted from the geophysical survey data by determining either a difference between positive and negative parts of the anomalies, or the difference from positive and background for smaller anomalies. This was performed using anomaly maps and Surfer grid files. The survey anomalies were measured at both the soil surface or at the gravel surface, depending upon data availability. The different distances of the sensor from the model dipole for the survey either at the soil or gravel surface were incorporated into the models by assuming the additional thickness of soil for the top-of-soil surveyed data (Table 9).

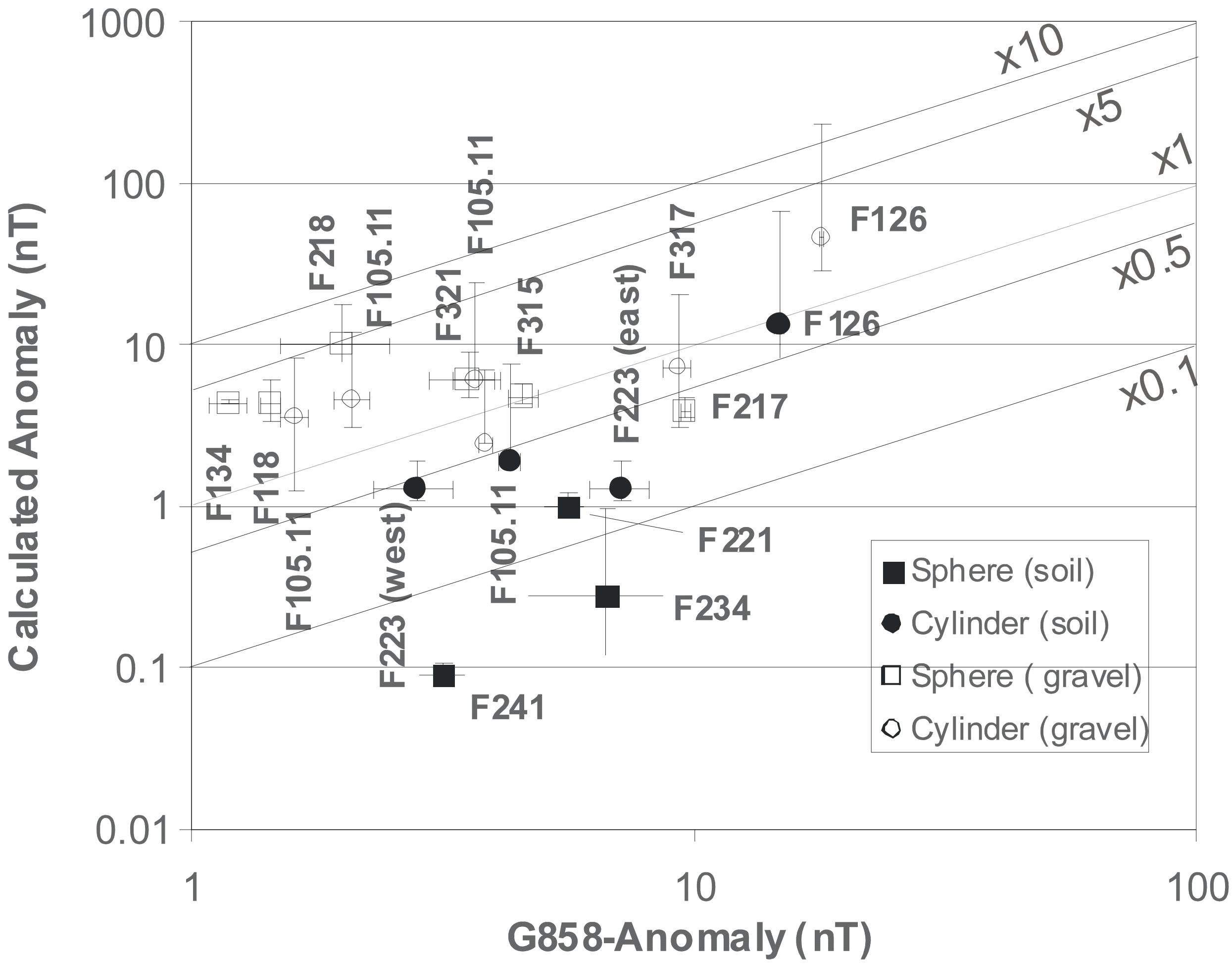

Figure 18. Calculated gradient anomaly versus the gradient anomaly determined with the G858 gradiometer. 'Error bars' for the calculated anomaly represent the 25% and 75% quartile values about the median value. Error bars on the measured anomaly represent the maximum and minimum range determined from the data points located over the anomaly peaks.

Most of the evaluated magnetic anomalies had been determined with the G858 gradiometer (Fig. 18). For the G858 magnetometer the anomalies calculated at soil-level are generally less than those measured by factors between about 0.9 and 0.03. Even allowing for the range of 25% to 75% quartile values only 2 out of the 7 determinations could be suggested to show reasonable correspondence between calculated and observed (Fig. 18). Those anomalies calculated for the gravel surface are generally larger by a factor of up to about 5 than those measured anomalies (although the calculated anomaly from feature F217 is consistently smaller than the measured value). Allowing for the range of 25% to 75% quartile values only 4 out of the 12 determinations show reasonable correspondence between calculated and observed . These differences are irrespective of the type of model used. For the FM256 gradiometer measured values are approximately the same as calculated, except for feature F141 (Fig. 19). The reasons for these differences are not entirely clear, but may include:

- Inadequate determination of the soil thickness, which may vary more significantly than the simple fixed value assumed here.
- Overestimation of appropriate material properties for some features in which only surface materials have been sampled. Based on the data in Fig. 8 this could give an overestimate of 2 to 8 times for some features. However, this is not applicable to all features. For example features F126 (although only some 10cm), F234, F317, F105.11, F324 and F223 do have vertical traverses of magnetic property specimens (Fig. 8, 18).
- Underestimation of the induced and remanent magnetisation of the Holocene sands, which form the 'background' for the magnetic contrast. Hence for some features such as F105.11, the magnetic susceptibility along the depth profile passes into the field-typical of the Holocene gravels and sands (Fig. 8). So that prior to its full feature depth, the material forming this fill will be indistinguishable from the magnetic average background . In the model this case would overestimate the volume of material contributing to the magnetic contrast.
- Magnetic models that are too simple in comparison to the varied morphology of the features. For example vertical (and lateral) changes in magnetic contrast cannot be accounted for in these simple models.
- The models predict the vertical field, whereas the G858 gradiometer measures the total field gradient, although this only provides a relatively small difference in the case of the Catholme site, because of the steep magnetic field.

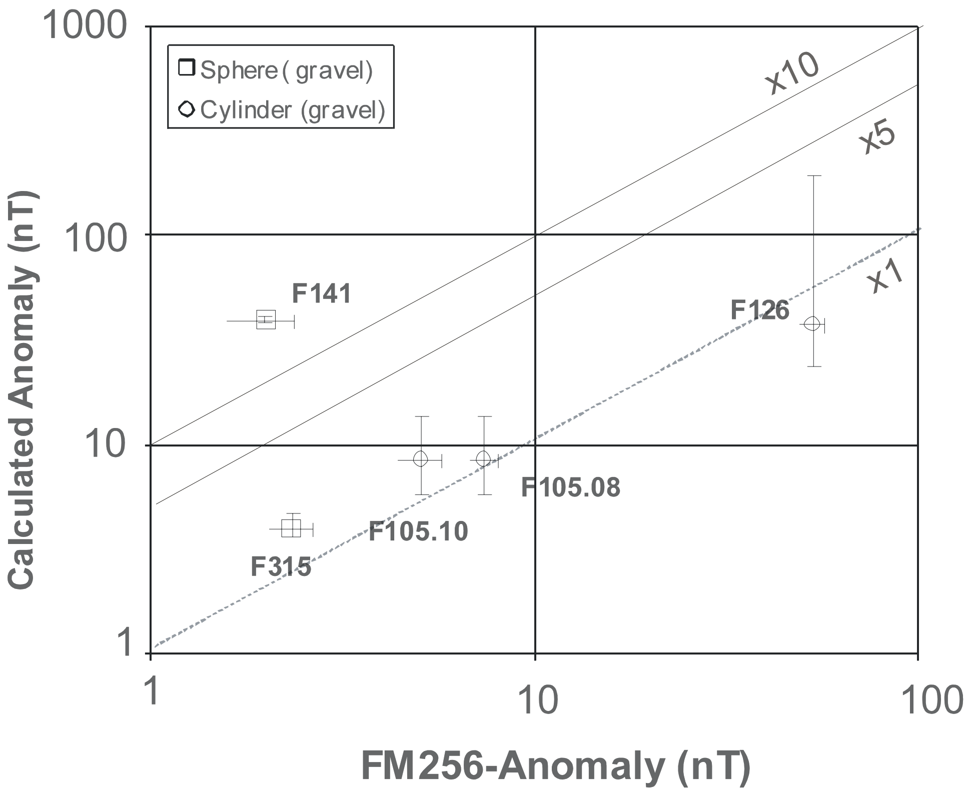

Fig. 19. *Calculated gradient anomaly versus the gradient anomaly determined with the FM256 gradiometer. 'Error bars' for the calculated anomaly represent the 25% and 75% quartile values about the median value. Error bars on the measured anomaly represent the maximum and minimum range determined from data points on the anomaly maps, about the mean value.*

7 Some reflection on the way forward

Two key questions remain about the magnetic properties of the Catholme site materials.

- Are the magnetic properties dominated by sources of burnt material?- as seem to be suggested by these initial environmental magnetic measurements. Validation of this should be sought by trying to find a relationship between charcoal content and the magnetic properties, and some experimental archaeology to determine the physical and magnetic fingerprint of what burnt site materials (soils, sands etc) should be like.
- Why is there such a poor relationship between magnetic material properties and the calculated magnetic anomalies? Is it a problem to do with the too simplistic models utilised here ? Is it that the 3-dimensional variability in magnetic properties is not properly characterised with the existing data set ? Detailed magnetic modelling focussed on specific strong anomaly features which have good material characterisation by a detailed 3-D program of magnetic susceptibility sampling of archaeological fill should be undertaken. This should also better characterise the 3-D variation in magnetic properties of the Holocene sands adjacent to the feature.

8 References

Butler, R.F. 1992. *Paleomagnetism, magnetic domains to geologic terranes*, Blackwell, Oxford, 319pp.

Clark, A. J., 1996. Seeing Beneath the Soil: Prospecting Methods in Archaeology (New Edition). B. T. Batsford Ltd., London.

Dearing, J.A., Hay, K.L. Baban, S.M.J., Huddleston, A.S., Wellington, E.M.H. and Loveland, P.J. 1996: Magnetic susceptibility of soil: An evaluation of conflicting theories using a national data set. *Geophysical Journal International* 127, 728–734.

Dunlop D., Özdemir Ö., 1997, Rock magnetism, Fundamentals and frontiers, Cambridge University Press, 573 pp.

Hounslow, M.W., & Chepstow-Lusty, A. 2002. Magnetic properties of charcoal rich deposits associated with a Roman bath house, Butrint (Southern Albania). Physics and Chemistry of the Earth, 27, 1333-1341.

Jordanova N., Jordanova J. and Karloukovski, V., 1996, Magnetic fabric of Bulgarian loess sediments derived by using various sampling techniques, Studia geophyisca et geodetica., 40, 36-49.

Jordanova, N., Petrovsky, E., Kovacheva, M & Jordanova, D. 2001. Factors determining magnetic enhancement of Burnt clay from archaeological sites. Journal. Archaeological Science, 28, 1137-1148.

Ketterings, Q.M., Bigham, J.M. and Laperche, V., 2000. Changes in soil mineralogy and texture caused by slash and burn fires in Sumatra, Indonesia. *Soil. Sci. Soc. Amer. Hour.*, 64, 1108-1117.

Kletetschka, G. and Banerjee, S.K., 1995. Magnetic stratigraphy of Chinese loess as a record of natural fires. *Geophys. Res. Lett.*, 22, 1341-1343, 1995.

Lu, H., Zhou, L. Han, J. Wu., N., Liu, T., Gu. Z., and Liu, B., 2000. Effect of burning C3 and C4 plants on the magnetic susceptibility signals in soils. *Geophys. Res. Lett.*, 27, 2031-2036.

Maher, B.A., Thompson, R. and Hounslow, M.W. 1999: Introduction, In Maher, B.A. and Thompson R., editors, *Quaternary climates, environments and magnetism*, Cambridge: Cambridge Univ. Press, 1–48.

NASA, 2004. IGRF Geomagnetic Field Model. http://nssdc.gsfc.nasa.gov/space/model/models/igrf.html [07/03/2005]

Peters, C. Thompson, R., Harrison, A. & Church, M.J. 2002. Low temperature characterization of fire-ash residues. Physics and Chemistry of the Earth, 27, 1355-1362.

Sharma, P.V., 1997. Environmental and engineering geophysics. Cambridge University press, Cambridge.

Thompson, R. and Oldfield, F., 1986. *Environmental magnetism*, Allen & Unwin, London.

Walden J., Oldfield, F. and Smith, J.P. (eds) 1999. Environmental Magnetism: a practical guide. Technical Guide, No 6, Quaternary Research Association, London.

Worm, H.U., 1998. On the superparamagnetic-stable single domain transition for magnetite, and frequency dependence of susceptibility, Geophys. J. Int., 133, 201-206.